DOI: 10.1002/ejoc.200901346

Supramolecular Assemblies Derived from Formyl-Substituted π-Conjugated Acyclic Anion Receptors

Hiromitsu Maeda,*[a,b] Rika Fujii,[a] and Yohei Haketa[a]

Keywords: Anions / Boron / Formyl units / Pyrrole derivatives / Receptors / Supramolecular chemistry

We report on the synthesis and properties of formyl-substituted dipyrrolyl diketone–BF_2 complexes (anion receptors) and their extended derivatives. The formyl-substituted receptors exhibited efficient anion-binding behavior and complicated solid-state hydrogen-bonding assembly patterns, due to the formyl group's electron-withdrawing and hydrogen-bond-accepting properties. The extended derivatives, prepared by the formation of Schiff bases and their subsequent reduction, behaved as building subunits to provide gel-like materials in spite of the existence of β-ethyl substituents. Fairly unspecific spherical particle morphologies were observed for these gel-like materials by optical microscopy and AFM. The anion-responsive behavior of the supramolecular assemblies (gelated materials) was also examined.

Introduction

Soft matter has been attracting increasing attention as a "transformable" functional material due to its moderate mobility and flexibility, which readily enable it to change its bulk shape and properties depending on the conditions.[1] Supramolecular gels are dimensionally controlled assemblies made up of low-molecular-weight (LMW) molecules held together by noncovalent interactions such as hydrogen bonding, metal coordination, van der Waals interaction, and π–π stacking. Gels derived from molecular assemblies, in which the components can be readily replaced with alternatives, may provide promising material systems for drug delivery and tissue engineering.[2,3] Supramolecular gels made up of molecules sensitive to external physical stimuli can be modulated and controlled by the conditions.[4] In contrast to physical stimuli, chemical stimuli such as the incorporation of a specific species can afford versatile supramolecular gels that change their states as a result of the interactions between the additives and the gelator molecules.[5] Of the various available chemical stimuli available, inorganic and biotic anions, such as halides, acetates, and phosphates, which are ubiquitous in biology, are essential, as can be seen in the activity of enzymes, transport of hormones, protein synthesis, and DNA regulation.[6,7] Recently, the chemistry of anion-responsive supramolecular gels has become all the more fascinating as a result of their potential as stimuli-responsive functional soft materials.[8,9]

Supramolecular gels based on metal complexes also exhibit transformation by anions.[9a–9c] Lee et al., for example, prepared a dendrimer-like oxyethylene-substituted bis(pyridine) derivative that forms coordination polymers or oligomers, such as dispersed helical structures and discrete cyclic conformations, through Ag^+ complexation; the morphologies of the organized structures depend on the counter anions present, such as NO_3^-, BF_4^-, and $CF_3SO_3^-$, without specific interactions with the gelators.[9a,9b] Aida et al. reported the synthesis of an alkyl-substituted pyrazole–Au^+ trinuclear complex that forms a red-emissive supramolecular hexane gel with states and emission behavior controlled by the anion-driven "liberation" of metal ions.[9c] Further, some of the amide- and urea-based supramolecular gels are anion-responsive because of the affinities of the polarized NH sites for anions, which disrupt the hydrogen-bond-assembled structures.[9d–9k] Under suitable conditions, the chemical stimuli not only act as inhibitors of the formation of supramolecular assemblies but also function as tuneable components that are included in the organized structures.

As efficient receptors for anions, we have reported acyclic planar π-conjugated systems in the form of BF_2 complexes of 1,3-dipyrrolylpropane-1,3-diones (e.g., **1a**–**c**, **2a**–**d**, Figure 1a),[10–12] which can bind anions through the action of two pyrrole NH moieties and the bridging CH system, with the inversion of the pyrrole rings (Figure 1b). In fact, α-aryl-substituted receptors containing long aliphatic chains (e.g., **1b**) form anion-responsive supramolecular organogels on gelation from octane solutions and exhibit transitions to the solution state on addition of appropriate anions,[8,12a] whereas amphiphilic receptors possessing hydrophilic chains (e.g., **1c**) form solvent-assisted assemblies, such as vesicular structures, in aqueous solution.[12d]

[a] College of Pharmaceutical Sciences, Institute of Science and Engineering, Ritsumeikan University
Kusatsu 525-8577, Japan
Fax: +81-77-561-2659
E-mail: maedahir@ph.ritsumei.ac.jp
[b] PRESTO, Japan Science and Technology Agency (JST)
Kawaguchi 332-0012, Japan

Supporting information for this article is available on the WWW under http://dx.doi.org/10.1002/ejoc.200901346.

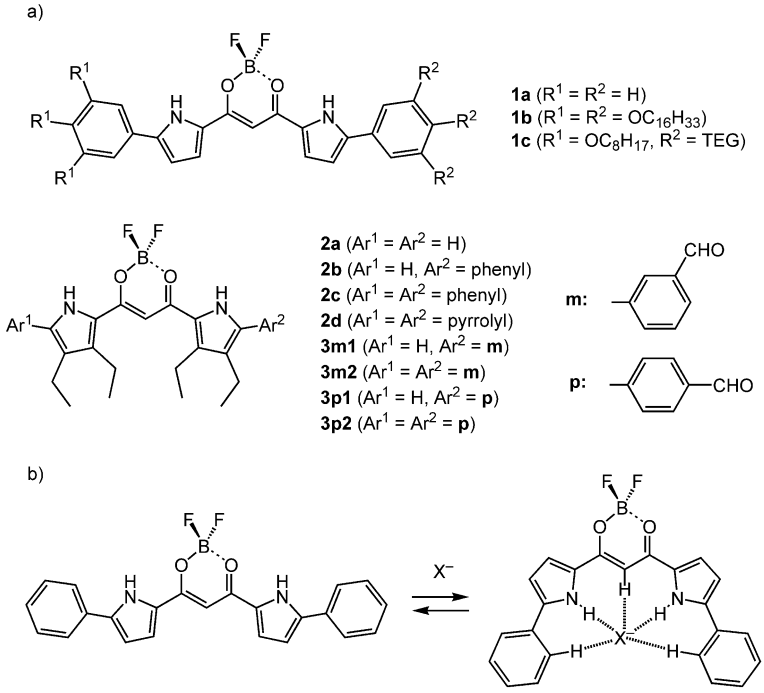

Figure 1. (a) BF_2 complexes of dipyrrolyl diketones **1a**–**c**, **2a**–**d**, and formyl-substituted derivatives (**3m1**, **3m2**, **3p1**, and **3p2**). (b) Anion-binding mode of **1a**.

Unlike the β-unsubstituted compounds **1a**–**c**, which are obtained from α-arylpyrroles as starting materials, the β-alkyl-substituted receptor **2a**, as an essential key starting material,[11e] can be converted into various π-extended receptors such as α-phenyl- (**2b**, **2c**) and α-pyrrolyl-substituted (**2d**) derivatives via α-iodinated intermediates.[12b,12c] Accordingly, the introduction of appropriate moieties that are readily transformable into other units would afford various anion-receptor derivatives. Of the potentially transformable groups, we chose the formyl (CHO) group, which is reactive for reduction to alcohols, oxidation to carboxylic acids, coupling to alkenes, condensation with amines to Schiff bases, etc.[13] In this paper we discuss formyl-substituted derivatives of the acyclic anion receptors (**3m1** and **3m2**, or **3p1** and **3p2**), which were converted into various derivatives that behaved as building blocks for supramolecular assemblies with/without anions in hydrocarbon solvents to afford gel-like materials. Effects of the sp^3-linkages between the core π-plane and the side aryl moieties are also discussed.

Results and Discussion

Synthesis and Characterization of BF_2 Complexes of Formyl-Substituted Dipyrrolyl Diketones

Mono- and diformyl substituents were introduced into acyclic anion receptors to yield the *meta*-monoformyl compound **3m1**, the *meta*-diformyl compound **3m2**, the *para*-monoformyl compound **3p1**, and the *para*-diformyl compound **3p2**, in 40, 44, 29, and 15% yields, respectively, through cross-coupling reactions with mono- and bis(α-iodo)-substituted BF_2 complexes[12b] and the corresponding (formylphenyl)boronic acid derivatives. The synthesis procedure with iodo-substituted receptors afforded better yields than those obtained with α-borylated dipyrrolyl diketones.[12d] The synthetic route starting from α-formylphenyl-substituted pyrrole and malonyl chloride, as in the case of **1a**–**c**,[12a] did not work well, possibly due to polymerization during the reactions to yield unidentified compounds. Chemical identification of **3m1**, **3m2**, **3p1**, and **3p2** was carried out by ^1H NMR and MALDI-TOF MS. The UV/Vis absorption bands of **3m1**, **3m2**, **3p1**, and **3p2** in CH_2Cl_2 were observed at 474, 495, 482, and 510 nm, respectively, suggesting that the formyl substitution at the *para* position extended the π-conjugation, whereas that at the *meta* position disrupted the π-conjugation to some extent, comparable to the situation with α-unsubstituted **2a** (451 nm),[11e] mono-α-phenylsubstituted **2b** (476 nm), and bis(α-phenyl)-substituted **2c** (499 nm).[12b] The order of these λ_{max} values was correlated to the order of the HOMO–LUMO gaps (**3m1**: 3.300 eV; **3m2**: 3.191 eV; **3p1**: 2.844 eV; **3p2**: 3.163 eV) as estimated by DFT calculations (Figures S3 and S4 in the Supporting Information).[14] Further, fluorescence emissions (and quantum yields Φ_F) excited at each absorption maximum in CH_2Cl_2 were observed at 504 (0.92) (**3m1**), 532 (0.98) (**3m2**), 511 (0.95) (**3p1**), and 547 nm (0.97) (**3p2**), suggesting that the formyl-substituted derivatives, like **2b** (Φ_F = 0.70) and **2c** (0.94), were also highly emissive fluorophores.

The solid-state structures of **3m1**, **3m2**, **3p1**, and **3p2** were determined by single-crystal X-ray analyses (Figure 2). All the receptor molecules formed hydrogen-bonding assemblies through their CHO moieties, along with the pyrrole NH and BF units. Here we have labeled the distances (C=)O···

(H–)N, (C=)O···(H–)*o*-C, F···(H–)C(=O), F···(H–)*o*-C, and F···(H–)N as *a*, *b*, *c*, *d*, and *e*, respectively. The monoformyl compound **3m1** formed hydrogen-bonding dimers with (C=)O···(H–)N and (C=)O···(H–)*o*-C distances of 2.963 (*a*)/3.418 (*a*′) and 3.080 (*b*)/3.331 (*b*′) Å, respectively. The B–F···H–C(=O) interaction [F···(H–)C(=O): 3.486 (*c*)/3.301 (*c*′) Å] also supported the assembled dimer structure (Figure 3a). On the other hand, the receptors **3m2**, **3p1**, and **3p2** exhibited the formation of 1-D hydrogen-bonding chain structures.

In the case of **3m2**, the (C=)O···(H–)N, (C=)O···(H–)*o*-C, and F···(H–)C(=O) distances in the chain structures were 3.075 (*a*)/3.029 (*a*′), 3.121 (*b*)/3.163 (*b*′), and 3.400 (*c*)/3.436 (*c*′) Å, respectively. The two formyl units in the receptor displayed inequivalent interaction, as observed in the hydrogen bond lengths (Figure 3b). The derivative **3m1** formed fairly planar supramolecular assemblies, which were efficient stacking structures. Interestingly, the monoformyl compound **3p1** produced 1-D chains through C=O···H–N interactions, which further constructed "knit"-like assemblies through B–F···H–N and B–F···H–*o*-C hydrogen bonding. The (C=)O···(H–)N, F···(H–)*o*-C, and F···(H–)N distances were 2.888 (*a*), 3.300 (*d*), and 3.235 (*e*) Å, respectively. A dihedral angle of 117.9° was observed between the two neighboring units (core π-planes) in the 1-D chains formed by C=O···H–N interactions (Figure 3c). The "center" molecules in this figure formed hydrogen-bonding assemblies through F···(H–)*o*-C and F···(H–)N with another C=O···H–N-based 1-D chain. Furthermore, the (C=)O···(H–)N, (C=)O···(H–)*o*-C, and F···(H–)C(=O) distances in **3p2** were 2.826 (*a*)/2.856 (*a*′), 3.248 (*b*)/3.113 (*b*′), and 3.426 (*c*)/3.301 (*c*′) Å, respectively. "Disordered" molecules formed 1-D chain structures through CHO units [Figure 3d(i)], whereas one of the CHO units of a molecule without a disordered structure [right in Figure 3d(ii)] served to associate with the hydrogen-bonding sites of the disordered molecule [left in Figure 3d(ii)]. The remaining hydrogen-bonding sites were partially associated with water molecules.

These formyl-substituted receptors had slightly distorted side aryl rings: the dihedral angles (minimum and maximum values) between the aryl rings and the dipyrrolyl core plane comprising 16 atoms were 27.5° and 30.7° for **3m1** (two independent structures), 29.2°/31.5° for **3m2**, 29.2° for **3p1**, and 33.1°/44.0° and 32.4°/44.1° for **3p2** (two independent structures). These values were comparable to or slightly larger than those in **2c** (24.3°/31.9°). The larger values were due to the intermolecular hydrogen bonding. The deviations in the mean plane consisting of 16 atoms were 0.26/0.35 Å (**3m1**), 0.20 Å (**3m2**), 0.37 Å (**3p1**), and 0.12/0.21 Å (**3p2**); these values are comparable to the value in **2c** (0.30 Å). Furthermore, as in other β-ethyl-substituted receptors,[11h,12b,12c] π–π stacking dimer structures were observed in the cases of **3m2** and **3p1** (Figure S2 in the Supporting Information), which had short distances of 3.774 (**3m2**) and 3.695 (**3p1**) Å. The longer distances of 4.085 (**3m2**) and 4.389 (**3p1**) Å between the stacking dimers suggested the influence of van der Waals interactions in stacking up the receptors. On the other hand, **3m1** gave infinite stacking assemblies, in which the parallel stacking distances were 3.600 and 3.994 Å and the nonparallel one was ca. 3.40 Å (estimated from the averaged distances from the 16

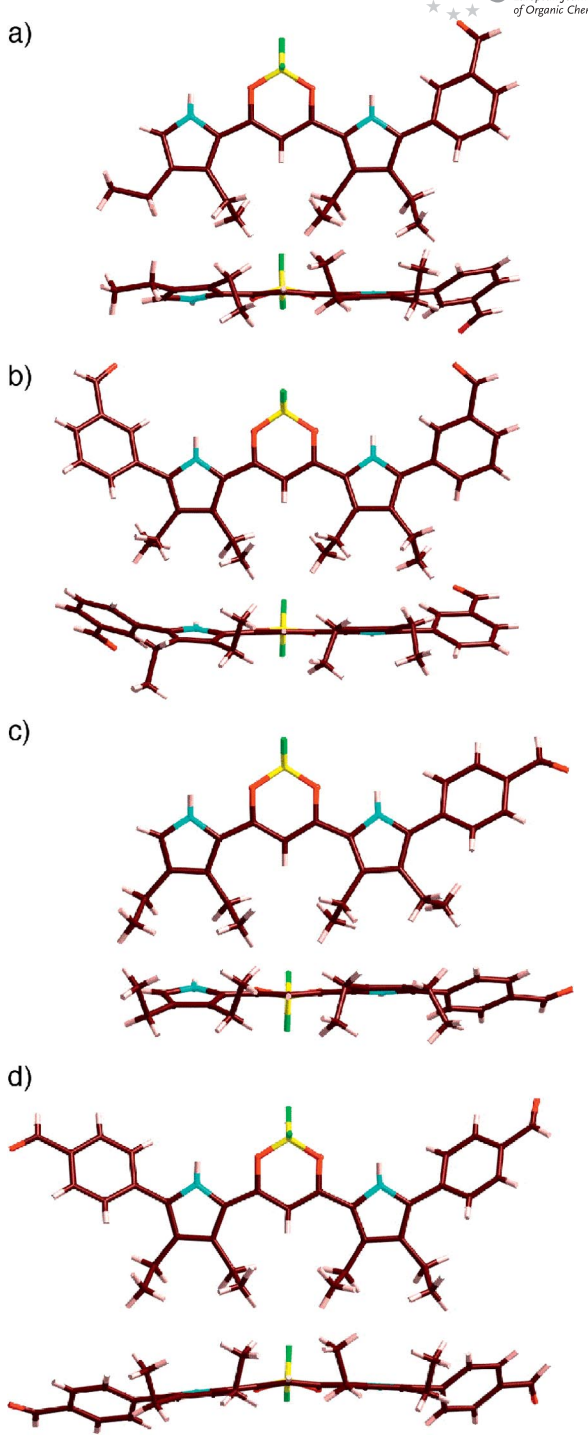

Figure 2. Single-crystal X-ray structures (top and side view) of: (a) **3m1** (one of the two independent structures), (b) **3m2**, (c) **3p1**, and (d) **3p2** (one of the two independent structures including a disordered pair). Atom color code: brown, pink, yellow, green, blue, and red refer to carbon, hydrogen, boron, fluorine, nitrogen, and oxygen, respectively. See also Figure S1 in the Supporting Information.

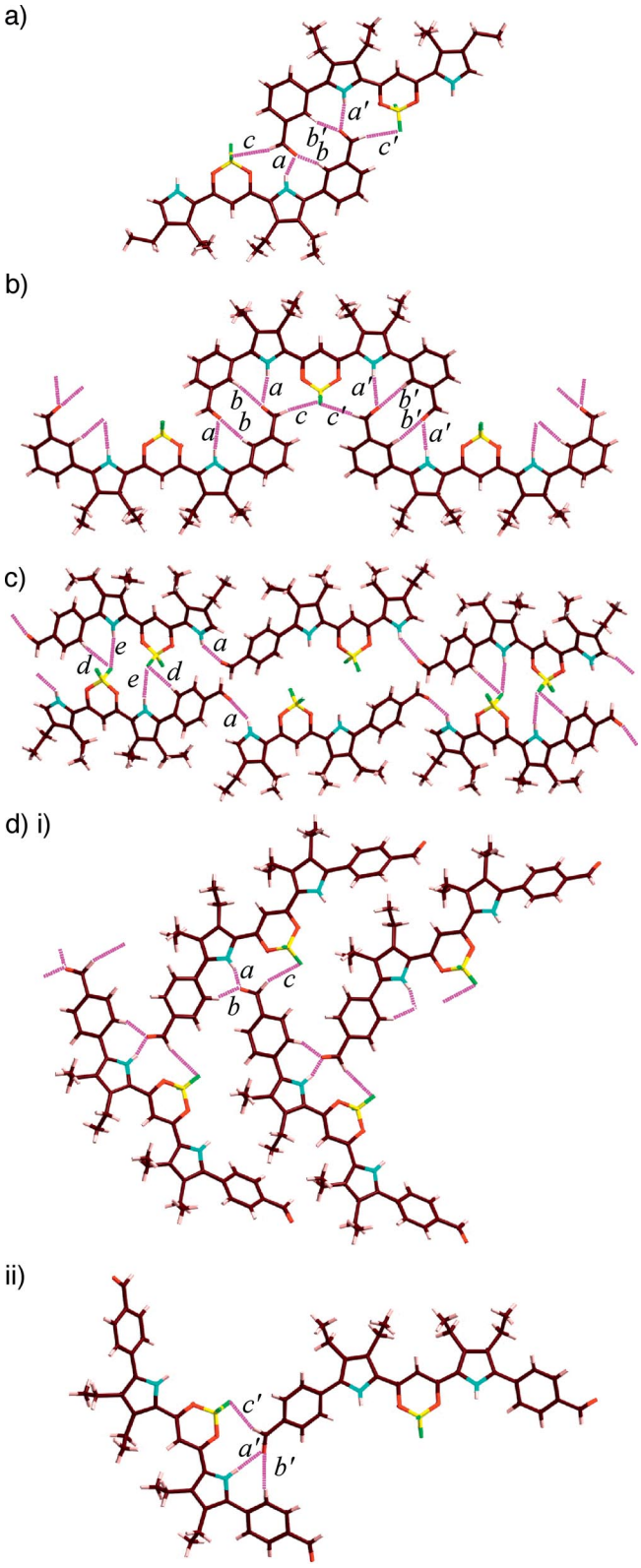

Figure 3. Hydrogen-bonding assemblies of (a) **3m1**, (b) **3m2**, (c) **3p1**, and (d) **3p2** in the solid state.

atoms of the receptor unit to the mean plane of the other unit). Relative to **3m2**, **3p1**, and other β-ethyl-substituted derivatives,[12b,12c,15] **3m1** exhibited a more tightly stacked structure comprising more than two units due to supporting van der Waals interactions between ethyl moieties and between ethyl units and the π-plane.

Anion-Binding Behavior of Formyl-Substituted Receptors

The values of the anion-binding constants (K_a) of **3m1**, **3m2**, **3p1**, and **3p2** (Table 1) were determined from the UV/Vis absorption spectral changes induced by the addition of appropriate anions, as their tetrabutylammonium (TBA) salts, in CH_2Cl_2 (Figures S6–S9 in the Supporting Information). The α-unsubstituted **2a** and the α-phenyl-substituted receptors **2b** and **2c** exhibited K_a values that decreased with increasing number of phenyl substituents, due to the steric hindrance between the α-phenyl and β-ethyl moieties.[12b] In contrast, the diformyl-substituted receptor **3m2** exhibited higher K_a values than the corresponding monoformyl compound **3m1**, whereas **3p2** showed larger K_a values than **3p1** for halide and $CH_3CO_2^-$ anions but slightly smaller K_a values for $H_2PO_4^-$ and HSO_4^-. This tendency in the formylphenyl-substituted receptors, in contrast with the phenyl-substituted receptors (**2b**, **2c**), was a result of the increased affinities of the *o*-CH sites in **3m1**, **3m2**, **3p1**, and **3p2** arising from the substitution with the electron-withdrawing formyl moiety.[16] The ^1H NMR spectral changes in **3m2** for anions such as Cl^- in CD_2Cl_2 suggested that the anions were bound to multiple binding sites of *o*-CH. Upon the addition of, for example, Cl^- (1.5 equiv.) to a CD_2Cl_2 solution of **3m2** (1×10^{-3} M) at –50 °C, the signals of the pyrrole NH, *o*-CH (two kinds), and bridging CH groups were shifted from δ = 9.60, 8.02/7.81, and 6.55 ppm to δ = 12.09 (chemical shift gap $\Delta\delta$ = 2.49 ppm), 8.35/8.13 ($\Delta\delta$ = 0.33/0.32), and 8.56 ($\Delta\delta$ = 2.01 ppm) ppm, respectively, suggesting that Cl^- was associated with the five hydrogen-bonding donor sites, as observed in **1a** and **2a**.[12a,12b] As well as the [1 (receptor) + 1 (anion)] complex, the [2 + 1] complex – with chemical shifts of NH (δ =10.87 ppm, $\Delta\delta$ = 1.27 ppm), CHO (δ =9.67 ppm, $\Delta\delta$ = –0.38 ppm from free receptor of δ = 10.05 ppm), *o*-CH (7.88/7.62 ppm, $\Delta\delta$ = –0.14/–0.19 ppm), and bridging CH (δ =7.48 ppm, $\Delta\delta$ = 0.93 ppm) – was also identified (Figure S12 in the Supporting Information).[17]

Substituted Aminomethyl Moieties from Formyl Groups to Enable the Receptors to Form Supramolecular Assemblies

The formyl group is well known to be transformable into imine (Schiff base) moieties by treatment with primary amines. The condensation of **3m1**, **3m2**, **3p1**, and **3p2** with hexadecylamine by general procedures was examined, and the formation of Schiff base products was detectable by MALDI-TOF MS. Isolation of the products was not easy, however, due to regeneration of starting materials by hydrolysis during silica gel column chromatography. Reduction of the Schiff base units with $NaBH(OAc)_3$ in the same pot as used for the condensation was therefore tried, and the formation of C–N single bonds worked well to sta-

Table 1. Binding constants (K_a [M^{-1}]) of **2a–c** (references), **3m1**, **3m2**, **3p1**, and **3p2** with various anions as TBA salts in CH_2Cl_2.[a]

	K_a(**2a**)[b]	K_a(**2b**)[c]	K_a(**2c**)[c]	K_a(**3m1**)	K_a(**3m2**)	K_a(**3p1**)	K_a(**3p2**)
Cl^-	6800	4200 (0.61)	2700 (0.40)	13000 (1.91)	27000 (4.0)	20000 (2.9)	65000 (9.6)
Br^-	1200	600 (0.50)	300 (0.25)	2000 (1.67)	2700 (2.3)	2200 (1.83)	3900 (3.3)
$CH_3CO_2^-$	210000	98000 (0.47)	27000 (0.13)	120000 (0.57)	200000 (0.95)	250000 (1.19)	320000 (1.5)
$H_2PO_4^-$	91000	36000 (0.40)	2200 (0.024)	9700 (0.11)	71000 (0.78)	74000 (0.81)	37000 (0.41)
HSO_4^-	1200	n.d.[d]	25 (0.021)	400 (0.33)	870 (0.73)	420 (0.35)	320 (0.27)

[a] The values in parentheses are the ratios of the K_a values to the K_a value of **2a**. [b] Ref.[11e] [c] Ref.[12b] [d] Not determined.

bilize the products **4m1**, **4m2**, **4p1**, and **4p2** as aminomethyl-substituted derivatives (Figure 4). The alkyl-substituted **4m1**, **4m2**, **4p1**, and **4p2** did not exhibit good solubility in hydrocarbon solvents such as octane.

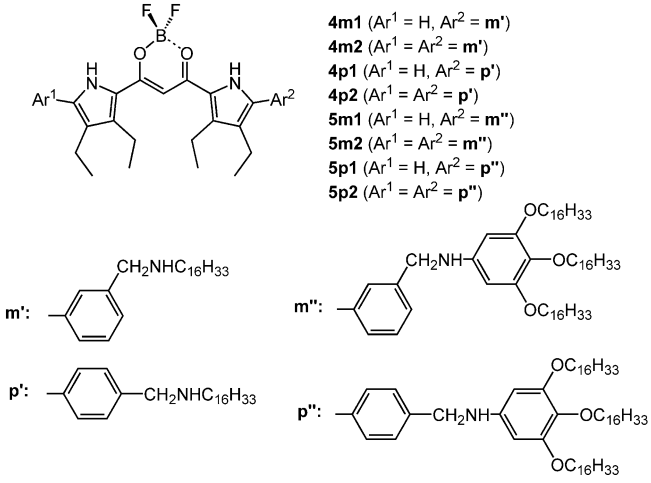

Figure 4. Extended derivatives **4m1**, **4m2**, **4p1**, **4p2**, **5m1**, **5m2**, **5p1**, and **5p2** from formyl-substituted **3m1**, **3m2**, **3p1**, and **3p2**.

As observed in the derivatives **4m1**, **4m2**, **4p1**, and **4p2**, imine formation and subsequent reduction reaction appeared to be useful for introduction of various substituents on either one or two sides of the acyclic anion receptors, and so we focused on derivatives that would be "soluble" in nonpolar solvents. The connection of aryl rings with aliphatic chains, for example, afforded building blocks for supramolecular assemblies based on π–π interaction at the core plane, along with van der Waals interactions of the side chains. In fact, the presence of bulky β-ethyl moieties often inhibited the formation of infinite π–π stacking structures but yielded "dimers," as suggested by the single-crystal X-ray analysis of **2a**. However, supporting van der Waals interactions between β-ethyl units (and π-planes), as observed in **3m1**, **3m2**, and **3p1**, were able to produce columnar structures under appropriate conditions. In view of the above observations, **3m1**, **3m2**, **3p1**, and **3p2** were transformed into **5m1**, **5m2**, **5p1**, and **5p2** (Figure 4) in yields of 54, 73, 64, and 64%, respectively, by treatment with 3,4,5-tris(hexadecyloxy)aniline[18] and subsequent $NaBH(OAc)_3$ reduction. The UV/Vis absorption bands of **5m1**, **5m2**, **5p1**, and **5p2** in CH_2Cl_2 (1×10^{-5} M) were observed at 478, 503, 480, and 505 nm, respectively, suggesting that only α-aryl substitution extended the π-conjugation observed in both *m*- and *p*-substituted receptors. The fluorescence emissions (and quantum yields Φ_F) of **5m1**, **5m2**, **5p1**, and **5p2** in CH_2Cl_2 were 510 (0.011), 536 (0.003), 515 (0.012), and 546 (0.007) nm, respectively. The low quantum yields were possibly the result of photoinduced electron transfer of amine lone pair(s). In contrast with their behavior in CH_2Cl_2, **5m1**, **5m2**, **5p1**, and **5p2** were "soluble" in octane at 1×10^{-5} M, possibly as stacking dimers and/or monomers, as suggested by fairly blueshifted UV/Vis absorption bands at 455, 484, 463, and 473 nm, respectively, wavelengths shorter by 23, 19, 17, and 32 nm than those seen in CH_2Cl_2. The fluorescence emissions (and quantum yields Φ_F) of **5m1**, **5m2**, **5p1**, and **5p2** in octane were observed at 488 (0.072), 519 (0.003), 492 (0.338), and 517 (0.114) nm, respectively (Figures S13 and S14 in the Supporting Information). The lower octane solubilities of the monosubstituted **5m1** and **5p1** at higher concentrations (ca. 10^{-3} M) were not appropriate for the formation of gel-like materials but afforded precipitates, and so in further studies we focused on the disubstituted **5m2** and **5p2**.[19]

The aliphatic derivative **1b**, which formed an octane gel below 27.5 °C (10 mg mL^{-1}),[12a] could be considered to be the "analogue" lacking the β-ethyl substituents and flexible aminomethyl-substituted phenyl moieties of **5m2** and **5p2**. Here we used octane as a solvent to construct supramolecular assemblies composed of **5m2** and **5p2**, as was attempted for **1b**. Unlike **1b**, **5m2** and **5p2** in octane (10 mg mL^{-1}) appeared to have fairly dispersed states, not gel-like ones, at room temp. When the solutions of **5m2** and **5p2** were cooled, they became opaque below ca. 1 and ca. –10 °C, respectively, and formed gel-like materials below ca. –10 and ca. –30 °C, respectively (Figure 5a).[20] Like the dispersed states in dilute octane solution, the gelated materials formed from **5m2** and **5p2** were less emissive but showed weak fluorescence (at around 595 and 517 nm for **5m2** and **5p2**, respectively) at room temp. The absorption maxima of **5m2** and **5p2** (10 mg mL^{-1}) at room temp. were observed at 485 and 470 nm, which were almost the same as the values in octane solutions at 1×10^{-5} M, in the dispersed states as stacking dimers and/or monomers. The variable-temperature (VT) UV/Vis spectral changes in **5m2** at 1×10^{-3} M between 60 and –50 °C exhibited the formation of stacking structures at lower temperatures: the absorption maxima were shifted from 482 (60 °C) to 487 nm (–40 °C), along with the augmentation of the shoulder at around 540 nm. Compound **5p2**, on the other hand, showed slightly complicated, two-step transitions: the band at 476 nm (60 °C) was shifted to 471 nm (0 °C) with a slightly augmented absorbance and, further, to 475 nm (–50 °C) as a broader and

weaker absorption. At this concentration (1×10^{-3} M), the absorbance at around 600–700 nm increased below –20 °C for **5m2** and **5p2**, suggesting that increases in absorbance at around 600–700 nm below –20 °C (Figure S15 in the Supporting Information) may be attributable to light scattering by larger objects, as observed in opaque solutions. The absorption spectra of solid-state compounds **5m2** and **5p2**, prepared from octane solutions (1×10^{-3} M) by air drying, with use of optical waveguides exhibited the assembled features of broad absorption bands with λ_{max} values of 452 and 441 nm, respectively, with shoulders at around 550 nm in both cases.

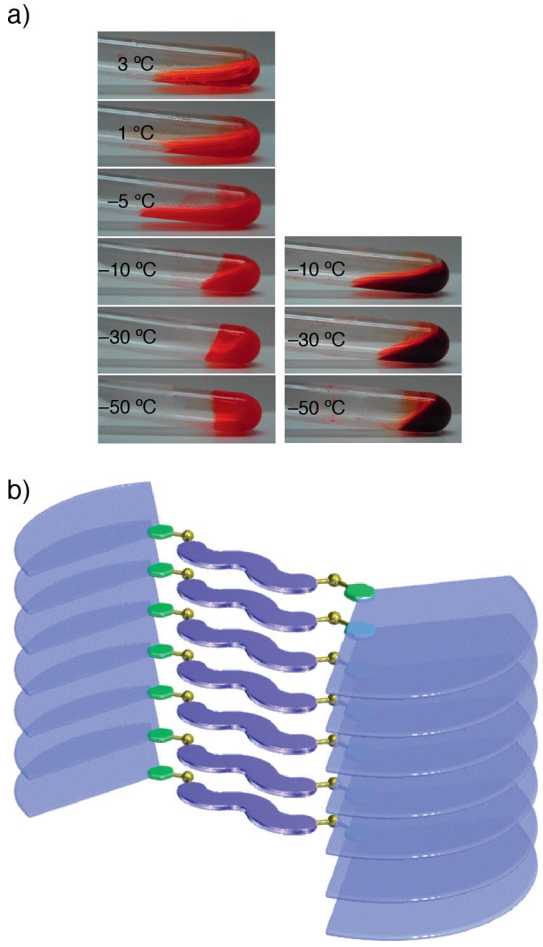

Figure 5. (a) Photographs of the gel-like materials formed from **5m2** (left) and **5p2** (right) in octane (10 mg mL^{-1}). (b) One of the possible assembling modes of **5m2** and **5p2**.

The morphologies of the organized structures of **5m2** and **5p2** were elucidated by optical microscopy (OM) and atomic force microscopy (AFM) measurements. Analytical samples of **5m2** and **5p2** (10 mg mL^{-1}) were prepared by drying gelated materials at –50 °C.[21] AFM measurements of the samples with use of glass and silicon substrates exhibited unspecific spherical morphologies with sizes of ca. 0.1–0.5 μm both for **5m2** and for **5p2** (see Figures S23a,b and 24a,b in the Supporting Information). Because gelated materials not derived from fibrous structures are rare,[4e,22] the spherical objects could possibly have been formed through the assembly and folding of relatively weak, thin stacking wires during the removal of the solvents. The fragile gel-like states were also suggested by the absence of any distinctions between the assembled features of **5m2** and **5p2**. The interconnection of three π-conjugated moieties, a core π-plane and two side aryl units, by an sp^3 methylene bridge (or bridges) provided supramolecular assemblies that were not very rigid but yielded soft materials through fairly ordered organization under appropriate conditions (Figure 5b).

VT ^{1}H NMR measurements of **5m2** and **5p2** (1×10^{-3} M) in [D_{18}]octane from 60 °C to –20 °C revealed the formation of aggregates at low temperatures (Figure 6). Both **5m2** and **5p2** showed broad but simple dispersed signals at 60 °C: in the case of **5p2**, for example, at δ = 9.60 (pyrrole-NH), 7.44 (core-aryl-CH), 6.37 (bridging CH), and 6.02 (terminal-aryl-CH) ppm. These observations suggested that the monomers were stable as major components at this temperature. At lower temperatures (0–40 °C for **5m2** and 0–20 °C for **5p2**), complicated features possibly derived from the formation of stacking dimers and/or other smaller assemblies were observed. At –20 °C, no signals ascribable to the formation of larger aggregates that were the basis of gelated materials at higher concentrations were observed.

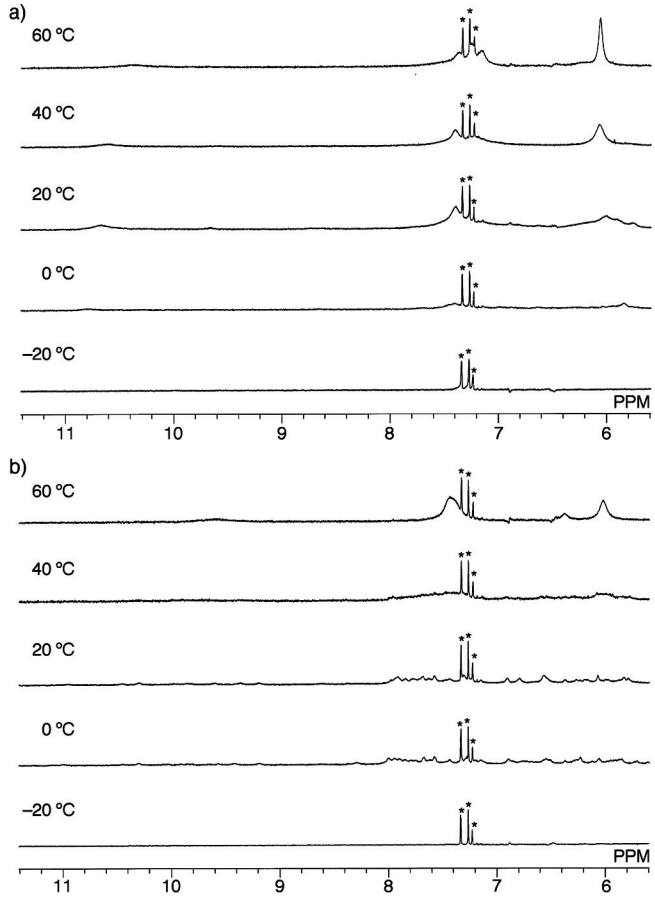

Figure 6. VT ^{1}H NMR spectral changes of (a) **5m2** and (b) **5p2** in [D_{18}]octane (1×10^{-3} M) from 60 °C to –20 °C. * Signals derived from solvents and solvent-related impurities.

The assembled behavior of **5m2** and **5p2** in *dilute* octane solutions (1×10^{-5} M and 1×10^{-4} M) was also examined by means of VT UV/Vis absorption spectral changes and compared to the behavior at 1×10^{-3} M (Figure 7 and Figure S16 in the Supporting Information). In the case of 1×10^{-5} M, a redshift from 482 to 491 nm was observed in **5m2** on cooling from 60 to –50 °C, and furthermore, increases in the absorbance at around 600–700 nm below –20 °C may also be attributable to the formation of larger objects. On heating from –50 to 60 °C, a reversible process was observed, although time-dependent absorption spectral changes at lower temperatures were also seen. Compound **5p2**, on the other hand, showed a blueshift from 484 to 477 nm on cooling from 60 to –50 °C, during which a decrease in absorbance due to the formation of assemblies was observed. At this concentration, the absorbance at around 600–700 nm increased below –20 °C for **5m2** and **5p2**. Similarly, measurements at 1×10^{-4} M showed spectral changes that indicated increased absorbance under –20 °C due to the formation of aggregates, along with some time-dependent behavior. There were no significant differences observed under these two sets of conditions. Furthermore, heating from room temp. to 60 °C at any concentration resulted in absorption changes, possibly due either to a transition from a stacking dimer to monomer or to changes in the stacking structures. From these results, which were basically similar to the features at 1×10^{-3} M, we identified the formation of organized structures resulting from the introduction of an aliphatic alkyl chain, as well as the effects of the substitution positions, even in dilute solutions.

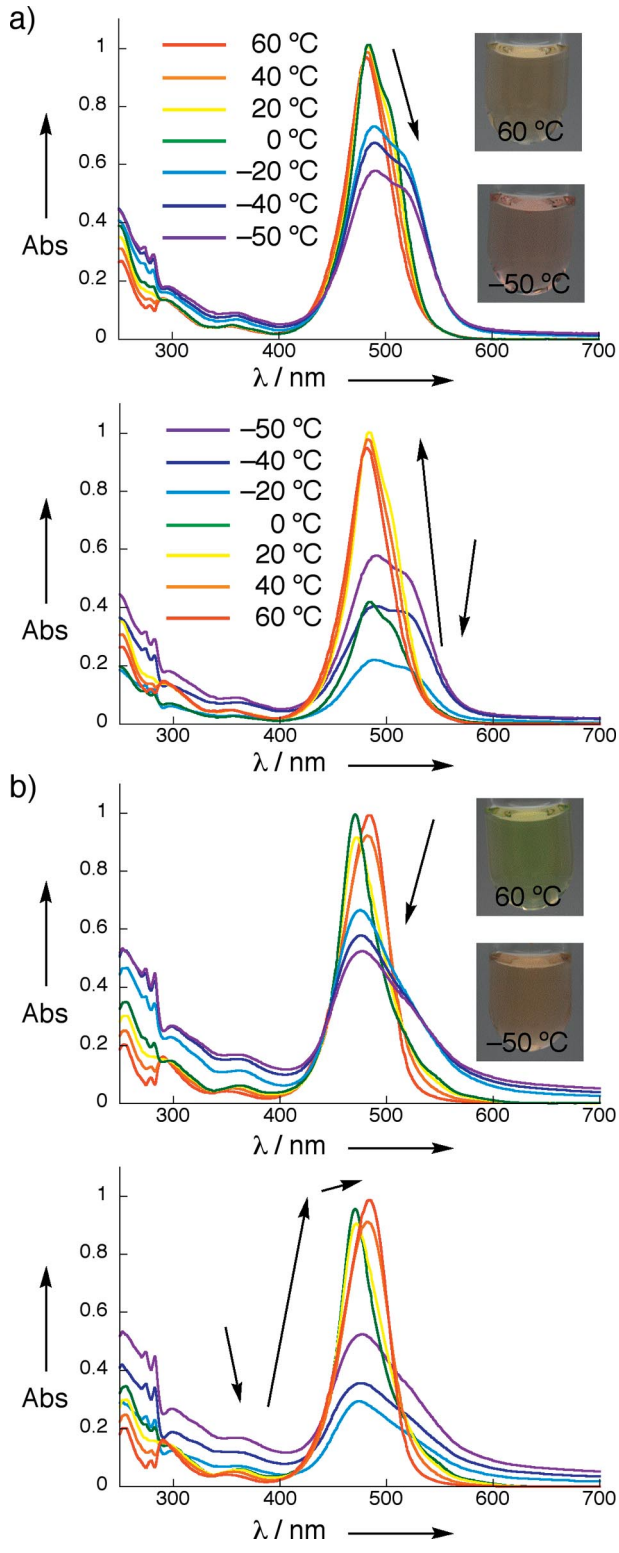

Figure 7. VT UV/Vis absorption spectral changes of (a) **5m2** and (b) **5p2** in octane (1×10^{-5} M) from 60 °C to –50 °C (top) and from –50 °C to 60 °C (bottom). Insets: Photographs at 60 and –50 °C.

Dynamic light scattering (DLS) measurements of **5m2** at 1×10^{-3} M exhibited mainly two diameter distributions at each temperature: 4 and 600 nm at 2 °C, 4 and 350 nm at 10 °C, 4 and 230 nm at 20 °C, 4 and 540 nm at 40 °C, and 3 and 100 nm at 80 °C. The smaller objects around 4 nm were presumably derived from the stacking of dimers and/or monomers,[23] whereas the larger ones may be small amounts of the higher aggregates. On the other hand, measurements at 1×10^{-4} M showed fairly random distributions at 2 and 10 °C and no DLS peaks at higher temperatures over 10 °C. Similarly, **5p2** showed only fairly random distributions or no peaks either at 1×10^{-3} M or at 1×10^{-4} M (Figure S20 in the Supporting Information).[24]

Anion-Responsive Behavior of Supramolecular Assemblies

Supramolecular assemblies made up of anion receptors (**5m2** and **5p2**) could be responsive and tuneable, because of the existence of anions. In fact, the addition of Cl^- (1 equiv.) as its TBA salt was capable of modulating the assembled structures, along with their optical and electronic properties; Cl^- complexes of both **5m2** and **5p2** in octane (10 mg mL^{-1}) were opaque solutions below ca. 5 °C and formed gel-like materials below ca. –10 °C (Figure 8), suggesting that the introduction of an anion also produced rigid organized structures, possibly due to the formation of assemblies consisting of alternately stacked positively and negatively charged species, as observed in the solid state with the Cl^- complexes of **1a** and **2d**.[12a,12c] Examination of the assembled structures containing TBACl was performed with the aid of AFM measurements on samples prepared

by drying at –50 °C on glass and silicon substrates, which revealed spherical morphologies with sizes of ca. 0.1–0.5 μm for the Cl^- complexes of **5m2** and **5p2** (Figures 23c,d and 24c,d in the Supporting Information).[21] The features of the Cl^- complexes were quite similar to those of anion-free **5m2** and **5p2**, presumably due to the fragilities of the assembled structures in the cases both of the receptors and of the anion complexes. The morphologies of the organized structures depended on the substitution positions of the terminal aryl rings, regardless of the presence of the TBA salt.

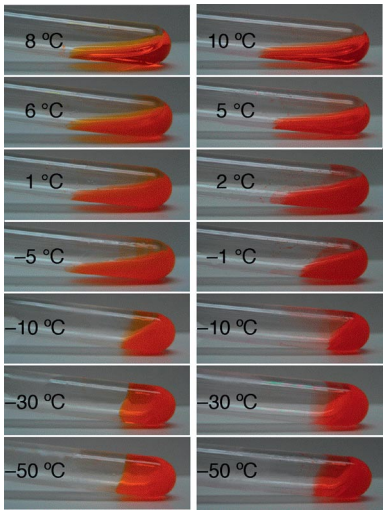

Figure 8. Photographs of the gel-like materials formed from **5m2** (left) and **5p2** (right) with Cl^- (1 equiv.) as a TBA salt in octane (10 mg mL^{-1}).

As under anion-free conditions, VT ^{1}H NMR measurements of the Cl^- complexes of **5m2** and **5p2** (1×10^{-3} M) in [D_{18}]octane also revealed the formation of aggregates at lower temperatures (Figure 9). The samples were prepared by addition of [D_{18}]octane to mixtures of the receptors and TBACl (1 equiv.), initially complexed in CH_2Cl_2, and the solvents were evaporated to dryness. The Cl^- complex of **5m2** exhibited fairly sharp signals as a monomeric complex at 60–20 °C: at 40 °C, **5m2**·Cl^- showed signals at δ = 12.18 (pyrrole-NH), 8.75 (bridging CH), and 8.66 (core-aryl-*o*-CH) ppm (Figure 9b). On the other hand, **5p2**·Cl^- showed broad and dispersed signals at 60–20 °C: at δ = 12.29 (pyrrole-NH), 8.94 (bridging CH), and 8.04 (core-aryl-*o*-CH) ppm at 40 °C, for example (Figure 9b). In neither case were signals observed at lower temperatures (0 to –20 °C), which is ascribable to the formation of larger aggregates, suggesting that such aggregates were produced directly from monomeric anion complexes. On the other hand, the VT UV/Vis absorption spectral changes in the Cl^- complexes of **5m2** and **5p2** (1×10^{-5} M) exhibited redshifts from 498 to 513 nm (**5m2**) and from 485 to 515 nm (**5p2**) on cooling from 60 to –50 °C (Figure 10 and Figures S17–S19 in the Supporting Information). Compounds **5m2** and **5p2** formed Cl^- complexes at all the temperatures used for measurements, as suggested by the relatively augmented and sharp bands at around 250–400 nm. The absorption spectra of **5m2** and **5p2** at above room temp. possibly originated from dispersed monomeric states, whereas those at lower temperatures were due to the assembled structures. The absorbance at around 600–700 nm increased below –20 °C with the formation of larger organized structures.

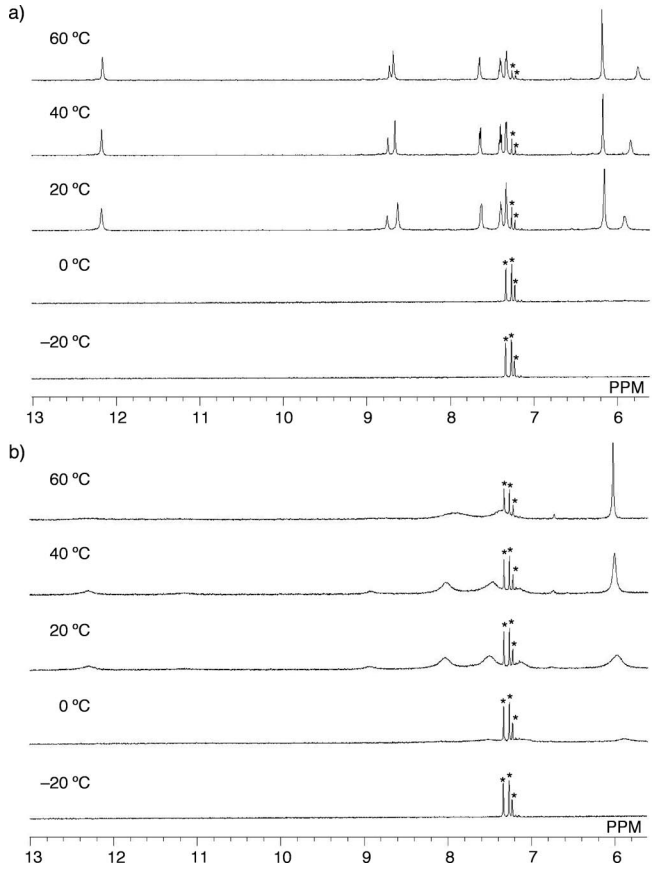

Figure 9. VT ^{1}H NMR spectral changes of (a) **5m2** and (b) **5p2** with Cl^- (1 equiv.) as its TBA salt in [D_{18}]octane (1×10^{-3} M) from 60 °C to –20 °C. * Signals derived from solvents and solvent-related impurities. The ^{1}H NMR anion-binding behavior is consistent with the UV/Vis absorption spectra of these materials (10 mg mL^{-1}) at room temp. (Figures S18h and S19h in the Supporting Information).

Complexation with an anion (Cl^-) afforded fairly sharp DLS peaks, presumably due to the formation of rigid assemblies consisting of charged species rather than those from anion-free receptors. Upon the addition of Cl^- (1 equiv.) as a TBA salt to an octane solution of **5m2** (1×10^{-3} M), a single distribution at 2000 nm was observed at 2 °C, whereas at 10–80 °C smaller assemblies at 2–5 nm, which were smaller at higher temperatures, and larger and fairly dispersed ones at 100–1000 nm were formed. The peak at 2–5 nm was from the result of the stacking of dimers and/or monomer, whereas the peaks at 2000 nm and around 100–1000 nm were due to the higher assembled structures. Compound **5p2** (1×10^{-3} M), on the other hand, which showed only random peaks in the absence of Cl^-, exhibited a larger but dispersed feature at 2 °C in the presence of Cl^- (1 equiv.), whereas at 10–80 °C temperature-dependent smaller peaks at 3–6 nm and larger ones at around 100–1000 nm were observed (Figure S21 in the Supporting

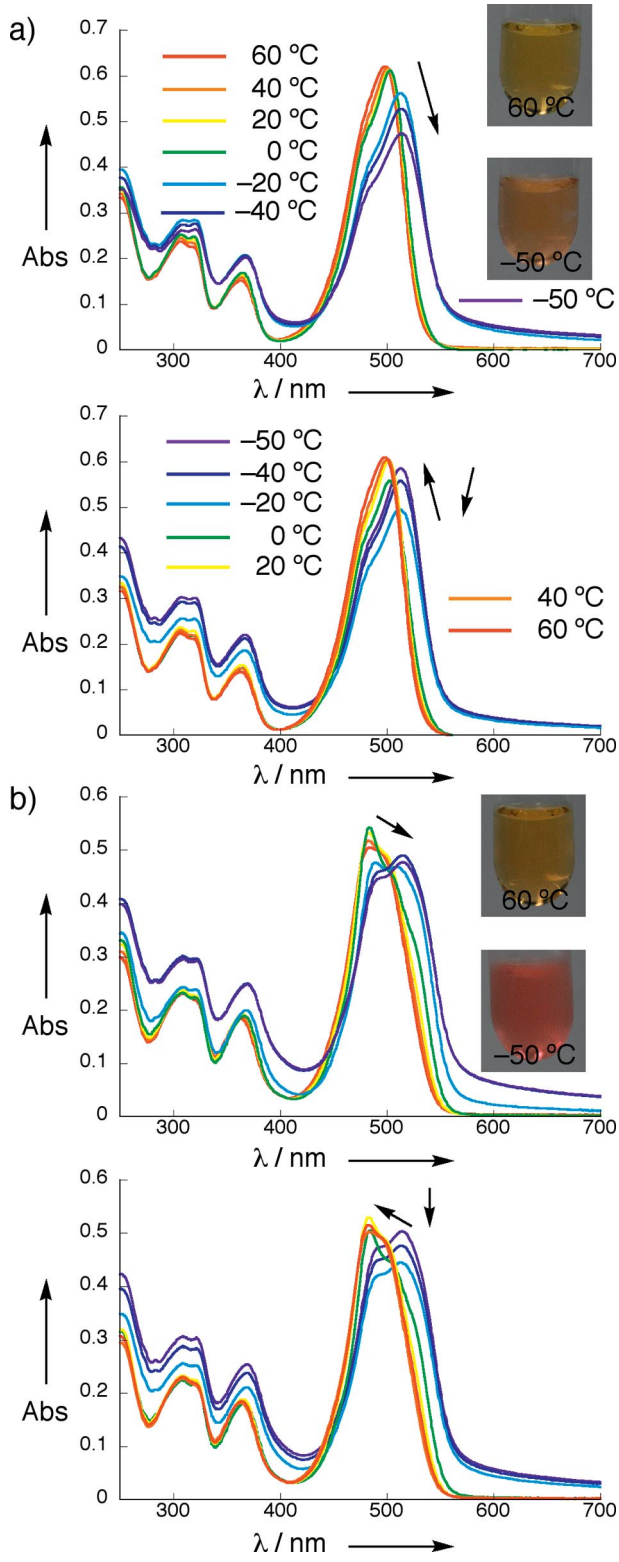

Figure 10. VT UV/Vis absorption spectral changes of (a) **5m2** and (b) **5p2** with Cl^- (1 equiv.) as its TBA salt in octane (1×10^{-5} M) from 60 °C to –50 °C (top) and from –50 °C to 60 °C (bottom). Insets: Photographs at 60 and –50 °C.

Information). At a lower concentration (1×10^{-4} M), **5m2** in the presence of Cl^- (1 equiv.) showed two distributions at around 4 and 400 nm at 10 °C, whereas **5p2** (1×10^{-4} M) in the presence of Cl^- (1 equiv.) showed distributions at 4 and 250 nm at 2 °C, 5 and 240 nm at 10 °C, and 4 and 400 nm at 20 °C. At over 40 °C, the peaks at around 4 nm were disordered and new ones representing larger assemblies appeared (Figure S22 in the Supporting Information).[24]

Conclusions

We have reported the synthesis and properties of formyl-substituted dipyrrolyl diketone–BF_2 complexes (anion receptors) and their extended derivatives. Formyl-substituted receptors exhibited efficient anion-binding behavior and complicated solid-state hydrogen-bonding assembly, due to the presence of additional hydrogen-bonding formyl moieties. The extended derivatives, which were prepared through the formation of Schiff bases and subsequent reduction, behaved as building subunits to provide gel-like materials responsive to anions. The synthesis of the other derivatives with the aid of formyl transformation and examination of their properties are now in progress.[25,26]

Experimental Section

General: Starting materials were purchased from Wako Chemical Co., Nacalai Chemical Co., and Aldrich Chemical Co. and were used without further purification unless otherwise stated. UV/Vis spectra were recorded with a Hitachi U-3500 spectrometer for the solution state and a System Instruments SIS-50 surface and interface spectrometer for the solid state. Variable-temperature UV/Vis spectra were measured with the aid of a Unisoku USP-203A cryostat for spectrophotometers. Fluorescence spectra and quantum yields were recorded with a Hitachi F-4500 fluorescence spectrometer for ordinary solutions and a Hamamatsu C9920-02 quantum yields measurements system for organic LED materials. NMR spectra used in the characterization of products were recorded with a JEOL ECA-600 600 MHz spectrometer. All NMR spectra were referenced to solvent. Matrix-assisted laser desorption ionization time-of-flight (MALDI-TOF) mass spectra were recorded with a Shimadzu Axima-CFRplus instrument in negative mode. Electrospray ionization mass spectrometry (ESI MS) studies were recorded with a Bruker microTOF instrument with use of a negative mode ESI-TOF method. TLC analyses were carried out on aluminium sheets coated with silica gel 60 (Merck 5554). Column chromatography was performed on Sumitomo alumina KCG-1525, Wakogel C-200, C-300, and Merck silica gel 60 and 60H.

BF_2 Complex of 1-[3,4-Diethyl-5-(3-formylphenyl)pyrrol-2-yl]-3-(3,4-diethylpyrrol-2-yl)propane-1,3-dione (3m1): A Schlenk tube containing the 5-iodo-substituted derivative of the bis(diethylpyrrolyl) diketone–BF_2 complex[12b] (49.1 mg, 0.10 mmol), *m*-formylphenylboronic acid (19.8 mg, 0.13 mmol), tetrakis(triphenylphosphane)palladium(0) (12.8 mg, 0.011 mmol), and Na_2CO_3 (42.2 mg, 0.40 mmol) was flushed with nitrogen and charged with a mixture of degassed DME (2 mL) and water (0.2 mL). The mixture was heated at 80 °C for 24 h, allowed to cool, and partitioned between water and CH_2Cl_2. The combined extracts were dried with anhydrous Na_2SO_4, and the solvents were evaporated to dryness. The residue was then chromatographed by silica gel flash column chromatography (MeOH/CH_2Cl_2, 1%), and crystallization from CH_2Cl_2/hexane afforded **3m1** (18.5 mg, 40%) as an orange solid. R_f = 0.48 (MeOH/CH_2Cl_2, 2%). ^1H NMR (600 MHz, $CDCl_3$,

20 °C): δ = 10.10 (s, 1 H, CHO), 9.42 (br., 1 H, NH), 9.34 (br., 1 H, NH), 8.02 (s, 1 H, ArH), 7.92 (d, J = 7.8 Hz, 1 H, ArH), 7.78 (d, J = 7.8 Hz, 1 H, ArH), 7.67 (t, J = 7.8 Hz, 1 H, ArH), 6.97 (d, J = 3.0 Hz, 1 H, pyrrole-H), 6.53 (s, 1 H, CH), 2.85 (q, J = 7.8 Hz, 2 H, CH_2), 2.81 (q, J = 7.8 Hz, 2 H, CH_2), 2.63 (q, J = 7.8 Hz, 2 H, CH_2), 2.49 (q, J = 7.8 Hz, 2 H, CH_2), 1.34 (t, J = 7.8 Hz, 3 H, CH_3), 1.28 (t, J = 7.8 Hz, 3 H, CH_3), 1.23 (t, J = 7.8 Hz, 3 H, CH_3), 1.21 (t, J = 7.8 Hz, 3 H, CH_3) ppm. UV/Vis (CH_2Cl_2): λ_{max} ($\varepsilon \times 10^5$) = 474 nm (1.15 $M^{-1}cm^{-1}$). MALDI-TOF MS: m/z (%) = 465.4 (100) [M – H]$^-$, 466.2 (76). ESI-TOF MS (HR): calcd. for $C_{26}H_{28}BF_2N_2O_3$ [M – H]$^-$ 465.2171; found 465.2171.

BF_2 Complex of 1,3-Bis[3,4-diethyl-5-(3-formylphenyl)pyrrol-2-yl]-propane-1,3-dione (3m2): A degassed DME solution (15 mL) of the diiodo-substituted derivative of the bis(diethylpyrrolyl) diketone–BF_2 complex[12b] (601.7 mg, 0.98 mmol), *m*-formylphenylboronic acid (367.3 mg, 2.45 mmol), tetrakis(triphenylphosphane)palladium(0) (114.0 mg, 0.099 mmol), Na_2CO_3 (416.1 mg, 3.93 mmol), and water (1.5 mL) was heated at reflux under N_2 for 25 h, allowed to cool, and partitioned between water and CH_2Cl_2. The combined extracts were dried with anhydrous Na_2SO_4, and the solvents were evaporated to dryness. The residue was then chromatographed by silica gel flash column chromatography (MeOH/$CHCl_3$, 2%), and crystallization from CH_2Cl_2/hexane afforded **3m2** (159.9 mg, 44%) as a red solid. R_f = 0.43 (MeOH/CH_2Cl_2, 2%). ^{1}H NMR (600 MHz, $CDCl_3$, 20 °C): δ = 10.11 (s, 2 H, CHO), 9.45 (br., 2 H, NH), 8.04 (s, 2 H, ArH), 7.93 (d, J = 7.8 Hz, 2 H, ArH), 7.79 (d, J = 7.8 Hz, 2 H, ArH), 7.68 (t, J = 7.8 Hz, 2 H, ArH), 6.61 (s, 1 H, CH), 2.88 (q, J = 7.8 Hz, 4 H, CH_2), 2.65 (q, J = 7.8 Hz, 4 H, CH_2), 1.36 (t, J = 7.8 Hz, 6 H, CH_3), 1.22 (t, J = 7.8 Hz, 6 H, CH_3) ppm. UV/Vis (CH_2Cl_2): λ_{max} ($\varepsilon \times 10^5$) = 495.5 nm (1.19 $M^{-1}cm^{-1}$). MALDI-TOF MS: m/z (%) = 569.4 (100) [M – H]$^-$, 570.4 (86). ESI-TOF MS (HR): calcd. for $C_{33}H_{32}BF_2N_2O_4$ [M – H]$^-$ 569.2434; found 569.2434.

BF_2 Complex of 1-[3,4-Diethyl-5-(4-formylphenyl)pyrrol-2-yl]-3-(3,4-diethylpyrrol-2-yl)propane-1,3-dione (3p1): A degassed DME solution (10 mL) of the 5-iodo-substituted derivative of the bis(diethylpyrrolyl) diketone–BF_2 complex[12b] (224.9 mg, 0.46 mmol), *m*-formylphenylboronic acid (104.1 mg, 0.69 mmol), tetrakis(triphenylphosphane)palladium(0) (53.6 mg, 0.046 mmol), Na_2CO_3 (166.1 mg, 1.57 mmol), and water (1 mL) was heated at reflux under N_2 for 30 h, allowed to cool, and partitioned between water and CH_2Cl_2. The combined extracts were dried with anhydrous Na_2SO_4, and the solvents were evaporated to dryness. The residue was then chromatographed by silica gel flash column chromatography (MeOH/CH_2Cl_2, 1%), and crystallization from CH_2Cl_2/hexane afforded **3p1** (61.6 mg, 29%) as an orange solid. R_f = 0.52 (MeOH/CH_2Cl_2, 5%). ^{1}H NMR (600 MHz, $CDCl_3$, 20 °C): δ = 10.07 (s, 1 H, CHO), 9.40 (br., 1 H, NH), 9.34 (br., 1 H, NH), 7.99 (d, J = 7.8 Hz, 1 H, ArH), 7.69 (d, J = 7.8 Hz, 1 H, ArH), 6.99 (d, J = 3.0 Hz, 1 H, pyrrole-H), 6.56 (s, 1 H, CH), 2.85 (q, J = 7.2 Hz, 2 H, CH_2), 2.81 (q, J = 7.2 Hz, 2 H, CH_2), 2.66 (q, J = 7.2 Hz, 2 H, CH_2), 2.50 (q, J = 7.2 Hz, 2 H, CH_2), 1.33 (t, J = 7.2 Hz, 3 H, CH_3), 1.28 (t, J = 7.2 Hz, 3 H, CH_3), 1.23 (t, J = 7.2 Hz, 3 H, CH_3), 1.22 (t, J = 7.2 Hz, 3 H, CH_3) ppm. UV/Vis (CH_2Cl_2): λ_{max} ($\varepsilon \times 10^5$) = 482.5 nm (1.04 $M^{-1}cm^{-1}$). MALDI-TOF MS: m/z (%) = 465.2 (100) [M – H]$^-$, 466.2 (90). ESI-TOF MS (HR): calcd. for $C_{26}H_{28}BF_2N_2O_3$ [M – H]$^-$ 465.2171; found 465.2171.

BF_2 Complex of 1,3-Bis[3,4-diethyl-5-(4-formylphenyl)pyrrol-2-yl]-propane-1,3-dione (3p2): A degassed DME solution (15 mL) of the diiodo-substituted derivative of the bis(diethylpyrrolyl) diketone–BF_2 complex[12b] (616.7 mg, 1.08 mmol), *m*-formylphenylboronic acid (374.9 mg, 2.50 mmol), tetrakis(triphenylphosphane)palladium(0) (115.9 mg, 0.10 mmol), Na_2CO_3 (424.2 mg, 4.00 mmol), and water (1.5 mL) was heated at reflux under N_2 for 25 h, allowed to cool, and partitioned between water and CH_2Cl_2. The combined extracts were dried with anhydrous Na_2SO_4, and the solvents were evaporated to dryness. The residue was then chromatographed by silica gel flash column chromatography (MeOH/$CHCl_3$, 1%), and crystallization from CH_2Cl_2/hexane afforded **3p2** (93.3 mg, 15%) as a red solid. R_f = 0.43 (MeOH/CH_2Cl_2, 5%). ^{1}H NMR (600 MHz, $CDCl_3$, 20 °C): δ = 10.08 (s, 2 H, CHO), 9.44 (br., 2 H, NH), 8.01 (d, J = 7.8 Hz, 2 H, ArH), 7.70 (d, J = 7.8 Hz, 2 H, ArH), 6.63 (s, 1 H, CH), 2.88 (q, J = 7.2 Hz, 4 H, CH_2), 2.67 (q, J = 7.2 Hz, 4 H, CH_2), 1.36 (t, J = 7.2 Hz, 6 H, CH_3), 1.23 (t, J = 7.2 Hz, 6 H, CH_3) ppm. UV/Vis (CH_2Cl_2): λ_{max} ($\varepsilon \times 10^5$) = 510 nm (1.06 $M^{-1}cm^{-1}$). MALDI-TOF MS: m/z (%) = 569.3 (100) [M – H]$^-$, 570.3 (98). ESI-TOF MS (HR): calcd. for $C_{33}H_{32}BF_2N_2O_4$ [M – H]$^-$ 569.2434; found 569.2435.

BF_2 Complex of 1-{3,4-Diethyl-5-[3-(hexadecylaminomethyl)phenyl]pyrrol-2-yl}-3-(3,4-diethylpyrrol-2-yl)propane-1,3-dione (4m1): Compound **3m1** (9.4 mg, 0.02 mmol) and hexadecylamine (24.3 mg, 0.1 mmol) were mixed in 1,2-dichloroethane (0.8 mL) at room temperature under nitrogen for 1 h. Sodium triacetoxyborohydride (16.9 mg, 0.08 mmol) and AcOH (1 μL, 0.02 mmol) were added, and the mixture was stirred at room temperature for 4 h. The reaction mixture was quenched with aqueous saturated $NaHCO_3$ solution and partitioned between water and CH_2Cl_2. The combined extracts were dried with anhydrous Na_2SO_4, and the solvents were evaporated to dryness. The residue was then chromatographed by silica gel column chromatography (MeOH/CH_2Cl_2, 3%), and crystallization from CH_2Cl_2/hexane afforded **4m1** (3.2 mg, 23%) as an orange solid. R_f = 0.20 (MeOH/CH_2Cl_2, 2%). ^{1}H NMR (600 MHz, $CDCl_3$, 50 °C): δ = 10.19 (br., 2 H, NH), 7.78 (s, 1 H, ArH), 7.42 (d, J = 6.6 Hz, 1 H, ArH), 7.22 (s, 2 H, ArH), 6.94 (s, 1 H, CH), 6.83 (s, 1 H, pyrrole-H), 3.96 (s, 2 H, CH_2), 2.92–2.88 (m, 6 H, CH_2, NHCH_2), 2.63 (q, J = 7.2 Hz, 2 H, CH_2), 2.49 (q, J = 7.2 Hz, 2 H, CH_2), 1.77 (br., 2 H, NHCH$_2CH_2$), 1.33–1.16 [m, 38 H, $(CH_2)_{13}$, CH_3], 0.89 (t, J = 7.2 Hz, 3 H, CH_3) ppm (amino-NH signal is missing, possibly due to its broadening characteristics). UV/Vis (CH_2Cl_2): λ_{max} ($\varepsilon \times 10^5$) = 474.5 nm (0.71 $M^{-1}cm^{-1}$). MALDI-TOF MS: m/z (%) = 691.7 (100) [M]$^-$. ESI-TOF MS (HR): calcd. for $C_{42}H_{63}BF_2N_3O_2$ [M – H]$^-$ 690.4994; found 690.4994.

BF_2 Complex of 1,3-Bis{3,4-diethyl-5-[3-(hexadecylaminomethyl)-phenyl]pyrrol-2-yl}propane-1,3-dione (4m2): Compound **3m2** (11.5 mg, 0.02 mmol) and hexadecylamine (48.1 mg, 0.2 mmol) were mixed in 1,2-dichloroethane (0.8 mL) at room temperature under nitrogen for 3 h. Sodium triacetoxyborohydride (25.8 mg, 0.12 mmol) and AcOH (2 μL, 0.04 mmol) were added, and the mixture was stirred at room temperature for 8 h. The reaction mixture was quenched with aqueous saturated $NaHCO_3$ solution and partitioned between water and CH_2Cl_2. The combined extracts were dried with anhydrous Na_2SO_4, and the solvents were evaporated to dryness. The residue was then chromatographed by silica gel column chromatography (MeOH/CH_2Cl_2, 5%), and crystallization from CH_2Cl_2/hexane afforded **4m2** (12.4 mg, 61%) as a red solid. R_f = 0.32 (MeOH/CH_2Cl_2, 5%). ^{1}H NMR (600 MHz, $CDCl_3$, 50 °C): δ = 9.94 (br., 2 H, NH), 8.35 (s, 2 H, ArH), 7.69 (d, J = 6.6 Hz, 2 H, ArH), 7.45 (t, J = 7.2 Hz, 2 H, ArH), 7.23 (d, J = 7.2 Hz, 2 H, ArH), 7.14 (s, 1 H, CH), 4.23 (s, 4 H, CH_2), 2.97 (q, J = 7.2 Hz, 4 H, CH_2), 2.84 (t, 4 H, NHCH_2), 2.72 (q, J = 7.2 Hz, 2 H, CH_2), 1.81 (br., 4 H, NHCH$_2CH_2$), 1.30–1.17 [m, 64 H, $(CH_2)_{13}$, CH_3], 0.88 (t, J = 7.2 Hz, 6 H, CH_3) ppm (amino-NH signal is missing possibly due to its broadening characteristics). UV/Vis (CH_2Cl_2): λ_{max} ($\varepsilon \times 10^5$) = 499.5 nm (0.60 $M^{-1}cm^{-1}$).

MALDI-TOF MS: *m*/*z* (%) = 1020.6 (100) $[M]^-$. ESI-TOF MS (HR): calcd. for $C_{65}H_{102}BF_2N_4O_2$ $[M - H]^-$ 1019.8080; found 1019.8080.

BF_2 Complex of 1-{3,4-Diethyl-5-[4-(hexadecylaminomethyl)phenyl]pyrrol-2-yl}-3-(3,4-diethylpyrrol-2-yl)propane-1,3-dione (4p1): Compound **3p1** (13.9 mg, 0.03 mmol) and hexadecylamine (37.1 mg, 0.15 mmol) were mixed in 1,2-dichloroethane (1.6 mL) at room temperature under nitrogen for 1 h. Sodium triacetoxyborohydride (31.8 mg, 0.15 mmol) and AcOH (2 μL, 0.04 mmol) were added, and the mixture was stirred at room temperature for 8 h. The reaction mixture was quenched with aqueous saturated $NaHCO_3$ solution and partitioned between water and CH_2Cl_2. The combined extracts were dried with anhydrous Na_2SO_4, and the solvents were evaporated to dryness. The residue was then chromatographed by silica gel column chromatography (MeOH/CH_2Cl_2, 4%) to afford **4p1** (15.6 mg, 77%) as an orange solid. R_f = 0.16 (MeOH/CH_2Cl_2, 2%). ^1H NMR (600 MHz, $CDCl_3$, 50 °C): δ = 9.31 (br., 2 H, NH), 7.47 (s, 4 H, ArH), 6.93 (d, *J* = 2.4 Hz, 1 H, pyrrole-H), 6.53 (s, 1 H, CH), 3.87 (s, 2 H, CH_2), 2.85 (q, *J* = 7.2 Hz, 2 H, CH_2), 2.81 (q, *J* = 7.2 Hz, 2 H, CH_2), 2.69 (t, *J* = 7.8 Hz, 2 H, NH*CH*$_2$), 2.62 (q, *J* = 7.2 Hz, 2 H, CH_2), 2.50 (q, *J* = 7.2 Hz, 2 H, CH_2), 1.58 (br., 2 H, $NHCH_2CH_2$), 1.33–1.16 [m, 38 H, $(CH_2)_{13}$, CH_3], 0.89 (t, *J* = 7.2 Hz, 3 H, CH_3) ppm (amino-NH signal is missing, possibly due to its broadening characteristics). UV/Vis (CH_2Cl_2): λ_{max} ($\varepsilon \times 10^5$) = 479 nm (1.07 $M^{-1}cm^{-1}$). MALDI-TOF MS: *m*/*z* (%) = 689.1 (40) $[M - H]^-$, 690.1 (100). ESI-TOF MS (HR): calcd. for $C_{42}H_{63}BF_2N_3O_2$ $[M - H]^-$ 690.4994; found 690.4994.

BF_2 Complex of 1,3-Bis{3,4-diethyl-5-[4-(hexadecylaminomethyl)phenyl]pyrrol-2-yl}propane-1,3-dione (4p2): Compound **3p2** (11.4 mg, 0.02 mmol) and hexadecylamine (48.4 mg, 0.2 mmol) were mixed in 1,2-dichloroethane (0.8 mL) at room temperature under nitrogen for 3 h. Sodium triacetoxyborohydride (34.2 mg, 0.16 mmol) and AcOH (2 μL, 0.04 mmol) were added, and the mixture was stirred at room temperature for 21 h. The reaction mixture was quenched with aqueous saturated $NaHCO_3$ solution and partitioned between water and CH_2Cl_2. The combined extracts were dried with anhydrous Na_2SO_4, and the solvents were evaporated to dryness. The residue was then chromatographed by silica gel column chromatography (MeOH/CH_2Cl_2, 10%) to afford **4p2** (12.0 mg, 59%) as a red solid. R_f = 0.51 (MeOH/CH_2Cl_2, 10%). ^1H NMR (600 MHz, $CDCl_3$, 20 °C): δ = 9.40 (s, 2 H, NH), 7.47 (s, 8 H, ArH), 6.51 (s, 1 H, CH), 3.84 (s, 4 H, CH_2), 2.84 (br., 4 H, CH_2), 2.68 (br., 4 H, NH*CH*$_2$), 2.60 (br., 4 H, CH_2), 1.58 (br., 4 H, $NHCH_2CH_2$), 1.32–1.16 [m, 64 H, $(CH_2)_{13}$, CH_3], 0.87 (t, *J* = 7.2 Hz, 6 H, CH_3) ppm (amino-NH signal is missing, possibly due to its broadening characteristics). UV/Vis (CH_2Cl_2): λ_{max} = 505 nm. MALDI-TOF MS: *m*/*z* (%) = 1018.9 (80) $[M - H]^-$, 1020.0 (100). ESI-TOF MS (HR): calcd. for $C_{65}H_{102}BF_2N_4O_2$ $[M - H]^-$ 1019.8080; found 1019.8080.

BF_2 Complex of 1-{3,4-Diethyl-5-[3-(3,4,5-trihexadecyloxyphenylaminomethyl)phenyl]pyrrol-2-yl}-3-(3,4-diethylpyrrol-2-yl)propane-1,3-dione (5m1): Compound **3m1** (4.6 mg, 0.01 mmol) and 3,4,5-trihexadecyloxyaniline (12.2 mg, 0.015 mmol) were mixed in 1,2-dichloroethane (0.4 mL) at room temperature under nitrogen for 2 h. Sodium triacetoxyborohydride (8.8 mg, 0.04 mmol) and AcOH (0.5 μL, 0.01 mmol) in 1,2-dichloroethane (0.1 mL) were added, and the mixture was stirred at room temperature for 20 h. The reaction mixture was quenched with aqueous saturated $NaHCO_3$ solution, and the product was extracted with CH_2Cl_2. The combined extracts were dried with anhydrous Na_2SO_4, and the solvents were evaporated to dryness. The residue was then chromatographed by silica gel column chromatography (MeOH/CH_2Cl_2, 2%), and crystallization from CH_2Cl_2/MeOH afforded **5m1** (6.8 mg, 54%) as an orange solid. R_f = 0.57 (MeOH/CH_2Cl_2, 1%). ^1H NMR (600 MHz, $CDCl_3$, 20 °C): δ = 9.34 (br., 1 H, NH), 9.29 (br., 1 H, NH), 7.51 (s, 1 H, ArH), 7.45–7.40 (m, 3 H, ArH), 6.94 (d, *J* = 3.6 Hz, 1 H, pyrrole-H), 6.51 (s, 1 H, CH), 5.87 (s, 2 H, ArH), 4.36 (s, 2 H, CH_2), 3.93 (s, 1 H, NH), 3.88 (t, *J* = 6.6 Hz, 4 H, *m*-OCH_2), 3.83 (t, *J* = 6.0 Hz, 2 H, *p*-OCH_2), 2.83 (q, *J* = 7.8 Hz, 2 H, CH_2), 2.79 (q, *J* = 7.8 Hz, 2 H, CH_2), 2.55 (q, *J* = 7.8 Hz, 2 H, CH_2), 2.49 (q, *J* = 7.8 Hz, 2 H, CH_2), 1.75–1.69 (m, 6 H, OCH_2CH_2), 1.44–1.39 (m, 6 H, $OCH_2CH_2CH_2$), 1.33–1.10 [m, 84 H, $(CH_2)_{12}$, CH_3], 0.87 (t, *J* = 7.8 Hz, 9 H, CH_3) ppm. UV/Vis (CH_2Cl_2): λ_{max} ($\varepsilon \times 10^5$) = 478 nm (0.99 $M^{-1}cm^{-1}$). MALDI-TOF MS: *m*/*z* (%) = 1263.5 (100) $[M - H]^-$, 1264.4 (82). ESI-TOF MS (HR): calcd. for $C_{80}H_{131}BF_2N_3O_5$ $[M - H]^-$ 1263.0168; found 1263.0166.

BF_2 Complex of 1,3-Bis{3,4-diethyl-5-[3-(3,4,5-trihexadecyloxyphenylaminomethyl)phenyl]pyrrol-2-yl}propane-1,3-dione (5m2): Compound **3m2** (22.8 mg, 0.04 mmol) and 3,4,5-trihexadecyloxyaniline (97.7 mg, 0.12 mmol) were mixed in 1,2-dichloroethane (2 mL) at room temperature under nitrogen for 3 h. Sodium triacetoxyborohydride (51.7 mg, 0.24 mmol) and AcOH (5 μL, 0.09 mmol) were added, and the mixture was stirred at room temperature for 20 h. The reaction mixture was quenched with aqueous saturated $NaHCO_3$ solution, and the product was extracted with CH_2Cl_2. The combined extracts were dried with anhydrous Na_2SO_4, and the solvents were evaporated to dryness. The residue was then chromatographed by silica gel column chromatography (MeOH/CH_2Cl_2, 2%), and crystallization from CH_2Cl_2/MeOH afforded **5m2** (63.0 mg, 73%) as a red solid. R_f = 0.68 (MeOH/CH_2Cl_2, 1%). ^1H NMR (600 MHz, $CDCl_3$, 20 °C): δ = 9.35 (s, 2 H, NH), 7.45–7.40 (m, 8 H, ArH), 6.55 (s, 1 H, CH), 5.88 (s, 4 H, ArH), 4.36 (s, 4 H, CH_2), 3.93 (s, 2 H, NH), 3.89 (t, *J* = 6.6 Hz, 8 H, *m*-OCH_2), 3.84 (t, *J* = 6.0 Hz, 4 H, *p*-OCH_2), 2.84 (q, *J* = 7.8 Hz, 4 H, CH_2), 2.56 (q, *J* = 7.8 Hz, 4 H, CH_2), 1.76–1.70 (m, 12 H, OCH_2CH_2), 1.44–1.39 (m, 12 H, $OCH_2CH_2CH_2$), 1.34–1.11 [m, 156 H, $(CH_2)_{12}$, CH_3], 0.88–0.86 (m, 18 H, CH_3) ppm. UV/Vis (CH_2Cl_2): λ_{max} ($\varepsilon \times 10^5$) = 503 nm (1.03 $M^{-1}cm^{-1}$). MALDI-TOF MS: *m*/*z* (%) = 2164.4 (70) $[M - H]^-$, 2165.5 (100). ESI-TOF MS (HR): calcd. for $C_{141}H_{238}BF_2N_4O_8$ $[M - H]^-$ 2165.8451; found 2165.8416.

BF_2 Complex of 1-{3,4-Diethyl-5-[4-(3,4,5-trihexadecyloxyphenylaminomethyl)phenyl]pyrrol-2-yl}-3-(3,4-diethylpyrrol-2-yl)propane-1,3-dione (5p1): Compound **3p1** (9.4 mg, 0.02 mmol) and 3,4,5-trihexadecyloxyaniline (24.4 mg, 0.03 mmol) were mixed in 1,2-dichloroethane (0.8 mL) at room temperature under nitrogen for 4 h. Sodium triacetoxyborohydride (17.5 mg, 0.08 mmol) and AcOH (1 μL, 0.02 mmol) were added, and the mixture was stirred at room temperature for 41 h. The reaction mixture was quenched with aqueous saturated $NaHCO_3$ solution, and the product was extracted with CH_2Cl_2. The combined extracts were dried with anhydrous Na_2SO_4, and the solvents were evaporated to dryness. The residue was then chromatographed by silica gel column chromatography (MeOH/CH_2Cl_2, 2%), and crystallization from CH_2Cl_2/MeOH afforded **5p1** (16.1 mg, 64%) as an orange solid. R_f = 0.48 (MeOH/CH_2Cl_2, 1%). ^1H NMR (600 MHz, $CDCl_3$, 20 °C): δ = 9.32 (br., 1 H, NH), 9.29 (br., 1 H, NH), 7.48 (s, 4 H, ArH), 6.95 (d, *J* = 2.4 Hz, 1 H, CH), 6.52 (s, 1 H, CH), 5.89 (s, 2 H, ArH), 4.33 (s, 2 H, CH_2), 3.90 (t, *J* = 6.6 Hz, 4 H, *m*-OCH_2; this peak overlaps the NH peak), 3.84 (t, *J* = 6.0 Hz, 2 H, *p*-OCH_2), 2.84 (q, *J* = 7.2 Hz, 2 H, CH_2), 2.80 (q, *J* = 7.8 Hz, 2 H, CH_2), 2.61 (q, *J* = 7.2 Hz, 2 H, CH_2), 2.49 (q, *J* = 7.8 Hz, 2 H, CH_2), 1.77–1.70 (m, 6 H, OCH_2CH_2), 1.44–1.43 (m, 6 H, $OCH_2CH_2CH_2$), 1.34–1.17

[m, 84 H, $(CH_2)_{12}$, CH_3], 0.87 (t, J = 7.2 Hz, 9 H, CH_3) ppm. UV/Vis (CH_2Cl_2): λ_{max} ($\varepsilon \times 10^5$) = 480 nm (1.10 $M^{-1}cm^{-1}$). MALDI-TOF MS: m/z (%) = 1263.2 (100) [M – H]$^-$, 1264.2 (83). ESI-TOF MS (HR): calcd. for $C_{80}H_{131}BF_2N_3O_5$ [M – H]$^-$ 1263.0168; found 1263.0167.

BF_2 Complex of 1,3-Bis{3,4-diethyl-5-[4-(3,4,5-trihexadecyloxyphenylaminomethyl)phenyl]pyrrol-2-yl}propane-1,3-dione (5p2): Compound **3p2** (22.7 mg, 0.04 mmol) and 3,4,5-trihexadecyloxyaniline (48.9 mg, 0.06 mmol) were mixed in 1,2-dichloroethane (0.8 mL) at room temperature under nitrogen for 21 h. Sodium triacetoxyborohydride (51.4 mg, 0.24 mmol) and AcOH (4.5 μL, 0.08 mmol) were added, and the mixture was stirred at room temperature for 24 h. The reaction mixture was quenched with aqueous saturated $NaHCO_3$ solution, and the product was extracted with CH_2Cl_2. The combined extracts were dried with anhydrous Na_2SO_4, and the solvents were evaporated to dryness. The residue was then chromatographed by silica gel column chromatography (MeOH/CH_2Cl_2, 2%), and crystallization from CH_2Cl_2/MeOH afforded **5p2** (55.2 mg, 64%) as a red solid. R_f = 0.68 (MeOH/CH_2Cl_2, 1%). ^{1}H NMR (600 MHz, $CDCl_3$, 20 °C): δ = 9.33 (s, 2 H, NH), 7.49 (s, 8 H, ArH), 6.56 (s, 1 H, CH), 5.89 (s, 4 H, ArH), 4.34 (s, 4 H, CH_2), 3.86 (t, J = 6.0 Hz, 8 H, m-OCH_2), 3.89 (s, 2 H, NH), 3.85 (t, J = 6.6 Hz, 4 H, p-OCH_2), 2.86 (q, J = 7.8 Hz, 4 H, CH_2), 2.62 (q, J = 7.8 Hz, 4 H, CH_2), 1.78–1.69 (m, 12 H, OCH_2CH_2), 1.45–1.41 (m, 12 H, $OCH_2CH_2CH_2$), 1.36–1.17 [m, 156 H, $(CH_2)_{12}$, CH_3], 0.88–0.86 (m, 18 H, CH_3) ppm. UV/Vis (CH_2Cl_2): λ_{max} ($\varepsilon \times 10^5$) = 506 nm (1.23 $M^{-1}cm^{-1}$). MALDI-TOF MS: m/z (%) = 2164.5 (80) [M – H]$^-$, 2165.5 (100). ESI-TOF MS (HR): calcd. for $C_{141}H_{238}BF_2N_4O_8$ [M – H]$^-$ 2165.8451; found 2165.8404.

Single-Crystal X-ray Analysis: Crystallographic data for **3m1**, **3m2**, **3p1**, and **3p2** are summarized in Table 2. A single crystal of **3m1** was obtained by vapor diffusion of hexane into a CH_2Cl_2 solution of **3m1**. The data crystal was a yellow prism. Data were collected with a Bruker CCD diffractometer and with use of graphite-monochromated Mo-K_α radiation; the structure was solved by direct methods. A single crystal of **3m2** was obtained by vapor diffusion of hexane into a $CHCl_3$ solution of **3m2**. The data crystal was a yellow prism. Data were collected with a Rigaku RAXIS-RAPID diffractometer and with use of graphite-monochromated Mo-K_α radiation; the structure was solved by direct methods. A single crystal of **3p1** was obtained by vapor diffusion of hexane into a $CHCl_3$ solution of **3p1**. The data crystal was a yellow prism. Data were collected with a Rigaku RAXIS-RAPID diffractometer and with use of graphite-monochromated Mo-K_α radiation; the structure was solved by direct methods. A single crystal of **3p2** was obtained by vapor diffusion of hexane into a $CHCl_3$ solution of **3p2**. The data crystal was a yellow prism. Data were collected with a Rigaku RAXIS-RAPID diffractometer and with use of graphite-monochromated Mo-K_α radiation; the structure was solved by direct methods. In each case, the non-hydrogen atoms were refined anisotropically. The calculations were performed with the aid of the Crystal Structure crystallographic software package from the Molecular Structure Corporation. CCDC-723260 (for **3m1**), -723261 (for **3m2**), -723262 (for **3p1**), and -723263 (for **3p2**) contain the supplementary crystallographic data for this paper. These data can be obtained free of charge from The Cambridge Crystallographic Data Centre via www.ccdc.cam.ac.uk/data_request/cif.

Atomic Force Microscopy (AFM): AFM measurements were carried out with an Olympus LEXT OLS3500 in dynamic force mode (tapping mode).

Methods for DLS: DLS measurements were determined by dynamic light scattering with a Malvern Zetasizer Nano-ZS instrument.

DFT Calculations: Ab initio calculations for **3m1**, **3m2**, **3p1**, and **3p2** and AM1 calculations for **5m2** and **5p2** were carried out with the aid of the Gaussian 03 program[14] and an HP Compaq dc5100 SFF computer. The structures for **3m1**, **3m2**, **3p1**, and **3p2** were optimized, and the total electronic energies were calculated at the B3LYP level by use of a 6-31G** basis set.

Supporting Information (see footnote on the first page of this article): X-ray crystallographic data (**3m1**, **3m2**, **3p1**, and **3p2**), opti-

Table 2. Crystallographic details for compounds **3m1**, **3m2**, **3p1**, and **3p2**.

	3m1	**3m2**	**3p1**	**3p2**
Empirical formula	$C_{26}H_{29}BF_2N_2O_3$	$C_{33}H_{33}BF_2N_2O_4{\cdot}CHCl_3$	$C_{26}H_{29}BF_2N_2O_3$	$C_{33}H_{33}BF_2N_2O_4{\cdot}0.66H_2O$
Molecular mass	466.32	689.79	466.32	581.05
Crystal size [mm]	0.45 × 0.20 × 0.05	0.50 × 0.30 × 0.20	0.50 × 0.30 × 0.10	0.80 × 0.40 × 0.20
Crystal system	triclinic	triclinic	monoclinic	monoclinic
Space group	$P\bar{1}$ (no. 2)	$P\bar{1}$ (no. 2)	$C2/c$ (no. 15)	$C2/c$ (no. 15)
a [Å]	12.525(2)	10.321(4)	17.711(6)	41.419(13)
b [Å]	14.885(3)	10.625(4)	9.322(3)	11.164(4)
c [Å]	15.601(3)	15.474(8)	28.431(10)	27.785(7)
α [°]	113.977(3)	74.619(17)	90	90
β [°]	113.436(3)	82.100(18)	101.648(15)	113.364(12)
γ [°]	94.245(3)	83.994(14)	90	90
V [Å^3]	2340.1(7)	1616.5(12)	4598(3)	11794(6)
ρ_{calcd} [g cm^{-3}]	1.324	1.417	1.347	1.309
Z	4	2	8	16
T [K]	90(2)	123(2)	123(2)	123(2)
μ(Mo-K_α) [mm^{-1}]	0.096	0.337	0.098	0.095
No. of reflections	11779	15525	21222	55377
No. of unique reflections	8059	7028	5240	13476
Variables	621	416	315	810
$\lambda_{Mo\text{-}K\alpha}$ [Å]	0.71073	0.71075	0.71075	0.71075
R_1 [$I > 2\sigma(I)$]	0.0917	0.0560	0.0498	0.0814
wR_2 [$I > 2\sigma$ (I)]	0.2143	0.1737	0.1269	0.2159
GOF	1.103	1.284	1.046	1.023

mized structures, anion-binding behavior, and supramolecular assemblies of formyl-substituted anion receptors and their derivatives.

Acknowledgments

This work was supported by Grants-in-Aid for Young Scientists (B) (No. 21750155) and for Scientific Research in a Priority Area "Super-Hierarchical Structures" (No. 18039038, 19022036) from the Ministry of Education, Culture, Sports, Science and Technology (MEXT) and the Ritsumeikan Global Innovation Research Organization (R-GIRO) project 2008-2013. The authors thank Prof. Atsuhiro Osuka, Dr. Shigeki Mori (currently at Ehime University), Mr. Shohei Saito, and Mr. Sumito Tokuji, Kyoto University, for X-ray analyses, Prof. Hiroshi Shinokubo and Dr. Satoru Hiroto, Nagoya University, for ESI MS measurements, and Prof. Hitoshi Tamiaki, Ritsumeikan University, for various measurements. Y. H. thanks the Japan Society for the Promotion of Science (JSPS) for a Research Fellowship for Young Scientists.

[1] a) J. N. Israelachvili, *Intermolecular and Surface Forces*, Academic Press, London, **1992**; b) I. W. Hamley, *Introduction to Soft Matter – Polymers, Colloids, Amphiphiles and Liquid Crystals*, John Wiley & Sons, Chichester, **2000**.

[2] a) *Low Molecular Mass Gelators*, *Topics in Current Chemistry* (Ed.: F. Fages), Springer-Verlag, Berlin, **2005**, vol. 256; b) T. Ishi-i, S. Shinkai, in *Supramolecular Dye Chemistry*, *Topics in Current Chemistry* (Ed.: F. Würthner), Springer-Verlag, Berlin, **2005**, vol. 258, pp. 119–160; c) *Molecular Gels* (Eds.: R. G. Weiss, P. Terech), Springer, Dordrecht, **2006**.

[3] a) P. Terech, R. G. Weiss, *Chem. Rev.* **1997**, *97*, 3133–3159; b) D. J. Abdallah, R. G. Weiss, *Adv. Mater.* **2000**, *12*, 1237–1247; c) J. H. van Esch, B. L. Feringa, *Angew. Chem.* **2000**, *112*, 2351–2354; *Angew. Chem. Int. Ed.* **2000**, *39*, 2263–2266; d) N. M. Sangeetha, U. Maitra, *Chem. Soc. Rev.* **2005**, *34*, 821–836.

[4] For example: a) J. J. D. de Jong, L. N. Lucas, R. M. Kellogg, J. H. van Esch, B. L. Feringa, *Science* **2004**, *304*, 278–281; b) M. Shirakawa, N. Fujita, S. Shinkai, *J. Am. Chem. Soc.* **2005**, *127*, 4164–4165; c) S. Yagai, T. Nakajima, K. Kishikawa, S. Kohmoto, T. Karatsu, A. Kitamura, *J. Am. Chem. Soc.* **2005**, *127*, 11134–11139; d) J. J. D. de Jong, T. D. Tiemersma-Wegman, J. H. van Esch, B. L. Feringa, *J. Am. Chem. Soc.* **2005**, *127*, 13804–13805; e) S. V. Aathimanikandan, E. N. Savariar, S. Thayumanavan, *J. Am. Chem. Soc.* **2005**, *127*, 14922–14929; f) T. Kitahara, M. Shirakawa, S.-i. Kawano, U. Beginn, N. Fujita, S. Shinkai, *J. Am. Chem. Soc.* **2005**, *127*, 14980–14981; g) S. Basu, D. R. Vutukuri, S. Thayumanavan, *J. Am. Chem. Soc.* **2005**, *127*, 16794–16795; h) T. Akutagawa, K. Kakiuchi, T. Hasegawa, S.-i. Noro, T. Nakamura, H. Hasegawa, S. Mashiko, J. Becher, *Angew. Chem.* **2005**, *117*, 7449–7453; *Angew. Chem. Int. Ed.* **2005**, *44*, 7283–7287; i) W. Weng, J. B. Beck, A. M. Jamieson, S. J. Rowan, *J. Am. Chem. Soc.* **2006**, *128*, 11663–11672; j) S. Matsumoto, S. Yamaguchi, S. Ueno, H. Komatsu, M. Ikeda, K. Ishizuka, Y. Ito, K. V. Tabata, H. Aoki, S. Ito, H. Noji, I. Hamachi, *Chem. Eur. J.* **2008**, *14*, 3977–3986; k) S. Matsumoto, S. Yamaguchi, A. Wada, T. Matsui, M. Ikeda, I. Hamachi, *Chem. Commun.* **2008**, 1545–1547.

[5] For example: a) K. Sugiyasu, N. Fujita, M. Takeuchi, S. Yamada, S. Shinkai, *Org. Biomol. Chem.* **2003**, *1*, 895–899; b) Y. Zang, H. Gu, Z. Yang, B. Xu, *J. Am. Chem. Soc.* **2003**, *125*, 13680–13681; c) N. Sreenivasachary, J.-M. Lehn, *Proc. Natl. Acad. Sci. USA* **2005**, *102*, 5938–5943; d) C. E. Stanley, N. Clarke, K. Anderson, M. J. A. Elder, J. T. Lenthall, J. W. Steed, *Chem. Commun.* **2006**, 3199–3201; e) C. Shi, J. Zhu, *Chem. Mater.* **2007**, *19*, 2392–2394; f) Z. Ge, J. Hu, F. Huang, S. Liu, *Angew. Chem.* **2009**, *121*, 1830–1834; *Angew. Chem. Int. Ed.* **2009**, *48*, 1798–1802; g) H. Komatsu, S. Matsumoto, S.-i. Tamaru, K. Kaneko, M. Ikeda, I. Hamachi, *J. Am. Chem. Soc.* **2009**, *131*, 5580–5585.

[6] a) *Supramolecular Chemistry of Anions* (Eds.: A. Bianchi, K. Bowman-James, E. García-España), Wiley-VCH, New York, **1997**; b) *Fundamentals and Applications of Anion Separations* (Eds.: R. P. Singh, B. A. Moyer), Kluwer Academic/Plenum Publishers, New York, **2004**; c) *Anion Sensing* (Ed.: I. Stibor), *Topics in Current Chemistry*, Springer-Verlag, Berlin, **2005**, vol. 255; d) J. L. Sessler, P. A. Gale, W.-S. Cho, *Anion Receptor Chemistry*, RSC, Cambridge, **2006**; e) *Recognition of Anions* (Ed.: R. Vilar), *Structure and Bonding*, Springer-Verlag, Berlin, **2008**.

[7] a) F. P. Schmidtchen, M. Berger, *Chem. Rev.* **1997**, *97*, 1609–1646; b) P. D. Beer, P. A. Gale, *Angew. Chem.* **2001**, *113*, 502–532; *Angew. Chem. Int. Ed.* **2001**, *40*, 487–516; c) R. Martínez-Mãnez, F. Sancenón, *Chem. Rev.* **2003**, *103*, 4419–4476; d) P. A. Gale, *Acc. Chem. Res.* **2006**, *39*, 465–475; e) P. A. Gale, R. Quesada, *Coord. Chem. Rev.* **2006**, *250*, 3219–3244; f) P. A. Gale, S. E. García-Garrido, J. Garric, *Chem. Soc. Rev.* **2008**, *37*, 151–190; g) C. Caltagirone, P. A. Gale, *Chem. Soc. Rev.* **2009**, *38*, 510–563.

[8] a) H. Maeda, *Chem. Eur. J.* **2008**, *14*, 11274–11282; b) G. O. Lloyd, J. W. Steed, *Nature Chem.* **2009**, *1*, 437–442.

[9] For example: a) H.-J. Kim, W.-C. Zin, M. Lee, *J. Am. Chem. Soc.* **2004**, *126*, 7009–7014; b) H.-J. Kim, J.-H. Lee, M. Lee, *Angew. Chem.* **2005**, *117*, 5960–5964; *Angew. Chem. Int. Ed.* **2005**, *44*, 5810–5814; c) A. Kishimura, T. Yamashita, T. Aida, *J. Am. Chem. Soc.* **2005**, *127*, 179–183; d) L. Applegarth, N. Clark, A. C. Richardson, A. D. M. Parker, I. Radosavljevic-Evans, A. E. Goeta, J. A. K. Howard, J. W. Steed, *Chem. Commun.* **2005**, 5423–5425; e) C. E. Stanley, N. Clarke, K. M. Anderson, J. A. Elder, J. T. Lenthall, J. W. Steed, *Chem. Commun.* **2006**, 3199–3201; f) J. E. A. Webb, M. J. Crossley, P. Turner, P. Thordarson, *J. Am. Chem. Soc.* **2007**, *129*, 7155–7162; Z. Dzoli'c, M. Cametti, A. D. Cort, L. Mandolini, M. Žini'c, *Chem. Commun.* **2007**, 3535–3537; g) C. Wang, D. Zhang, D. Zhu, *Langmuir* **2007**, *23*, 1478–1482; h) Q. Li, Y. Wang, W. Li, L. Wu, *Langmuir* **2007**, *23*, 8217–8223; i) H. Yang, T. Yi, Z. Zhou, Y. Zhou, J. Wu, M. Xu, F. Li, C. Huang, *Langmuir* **2007**, *23*, 8224–8230; j) M. Yamanaka, T. Nakamura, T. Nakagawa, H. Itagaki, *Tetrahedron Lett.* **2007**, *48*, 8990–8993; k) M.-O. M. Piepenbrock, G. O. Lloyd, N. Clarke, J. W. Steed, *Chem. Commun.* **2008**, 2644–2646.

[10] a) H. Maeda, *Eur. J. Org. Chem.* **2007**, 5313–5325; b) H. Maeda, *J. Incl. Phenom.* **2009**, *64*, 193–214.

[11] a) H. Maeda, Y. Kusunose, *Chem. Eur. J.* **2005**, *11*, 5661–5666; b) C. Fujimoto, Y. Kusunose, H. Maeda, *J. Org. Chem.* **2006**, *71*, 2389–2394; c) H. Maeda, Y. Ito, *Inorg. Chem.* **2006**, *45*, 8205–8210; d) H. Maeda, Y. Ito, Y. Kusunose, *Chem. Commun.* **2007**, 1136–1138; e) H. Maeda, Y. Kusunose, Y. Mihashi, T. Mizoguchi, *J. Org. Chem.* **2007**, *72*, 2612–2616; f) H. Maeda, M. Terasaki, Y. Haketa, Y. Mihashi, Y. Kusunose, *Org. Biomol. Chem.* **2008**, *6*, 433–436; g) H. Maeda, Y. Fujii, Y. Mihashi, *Chem. Commun.* **2008**, 4285–4287; h) H. Maeda, Y. Haketa, Y. Bando, S. Sakamoto, *Synth. Met.* **2009**, *159*, 792–796.

[12] a) H. Maeda, Y. Haketa, T. Nakanishi, *J. Am. Chem. Soc.* **2007**, *129*, 13661–13674; b) H. Maeda, Y. Haketa, *Org. Biomol. Chem.* **2008**, *6*, 3091–3095; c) H. Maeda, Y. Mihashi, Y. Haketa, *Org. Lett.* **2008**, *10*, 3179–3182; d) H. Maeda, Y. Ito, Y. Haketa, N. Eifuku, E. Lee, M. Lee, T. Hashishin, K. Kaneko, *Chem. Eur. J.* **2009**, *15*, 3709–3719; e) H. Maeda, N. Eifuku, *Chem. Lett.* **2009**, *38*, 208–209.

[13] *Organic Functional Group Preparations*, 2nd ed. (Eds.: S. R. Sandler, W. Karo), Academic Press, Inc., New York, **1983**.

[14] M. J. Frisch, G. W. Trucks, H. B. Schlegel, G. E. Scuseria, M. A. Robb, J. R. Cheeseman, J. A. Montgomery Jr., T. Vreven, K. N. Kudin, J. C. Burant, J. M. Millam, S. S. Iyengar, J. Tomasi, V. Barone, B. Mennucci, M. Cossi, G. Scalmani, N. Rega, G. A. Petersson, H. Nakatsuji, M. Hada, M. Ehara, K.

Toyota, R. Fukuda, J. Hasegawa, M. Ishida, T. Nakajima, Y. Honda, O. Kitao, H. Nakai, M. Klene, X. Li, J. E. Knox, H. P. Hratchian, J. B. Cross, C. Adamo, J. Jaramillo, R. Gomperts, R. E. Stratmann, O. Yazyev, A. J. Austin, R. Cammi, C. Pomelli, J. W. Ochterski, P. Y. Ayala, K. Morokuma, G. A. Voth, P. Salvador, J. J. Dannenberg, V. G. Zakrzewski, S. Dapprich, A. D. Daniels, M. C. Strain, O. Farkas, D. K. Malick, A. D. Rabuck, K. Raghavachari, J. B. Foresman, J. V. Ortiz, Q. Cui, A. G. Baboul, S. Clifford, J. Cioslowski, B. B. Stefanov, G. Liu, A. Liashenko, P. Piskorz, I. Komaromi, R. L. Martin, D. J. Fox, T. Keith, M. A. Al-Laham, C. Y. Peng, A. Nanayakkara, M. Challacombe, P. M. W. Gill, B. Johnson, W. Chen, M. W. Wong, C. Gonzalez, J. A. Pople, *Gaussian 03* (Revision C.01), Gaussian, Inc., Wallingford, CT, **2004**.

[15] The distances between π-planes in the β-ethyl-substituted derivatives in the solid state were 3.729 and 4.191 Å for α-phenyl compound **2c**, 3.378 and 5.011 Å for α-pyrrolyl compound **2d**, and 3.386 and 5.087 Å for the α-thienyl compound (not shown). On the other hand, α-H (**2a**) and α-furyl (not shown) formed only the stacking dimers without infinite columnar structures.

[16] The relative energies of the preorganized conformations with the inversion of two pyrrole rings, as appropriate for anion binding, were +3.59 (**3m1**), +2.69 (**3m2**), +5.21 (**3p1**), and +4.38 (**3p2**) kcal mol^{-1}, as calculated by DFT studies. These values showed almost no correlations with the binding affinities (K_a) for anions.

[17] The existence of the [2 + 1] complexes has already been confirmed in a previous report. See ref.[12a]

[18] V. Percec, M. R. Imam, T. K. Bera, V. S. K. Balagurusamy, M. Peterca, P. A. Heiney, *Angew. Chem.* **2005**, *117*, 4817–4823; *Angew. Chem. Int. Ed.* **2005**, *44*, 4739–4745.

[19] The binding constants (K_a values) of **5p2** in CH_2Cl_2 were 6100 (Cl^-), 560 (Br^-), 42000 ($CH_3CO_2^-$), 7000 ($H_2PO_4^-$), and 20 M^{-1} (HSO_4^-) (Figure S10 in the Supporting Information), which were similar to the values of **2c**. Therefore, the effect of the aminomethyl substituents did not seem very significant.

[20] For selected recent examples of temperature-dependent stacking assemblies, see: a) P. Jonkheijm, P. van der Schoot, A. P. H. J. Schenning, E. W. Meijer, *Science* **2006**, *313*, 80–84; b) X.-Q. Li, V. Stepanenko, Z. Chen, P. Prins, L. D. A. Siebbeles, F. Würthner, *Chem. Commun.* **2006**, 3871–3873; c) F. J. M. Hoeben, M. Wolffs, J. Zhang, S. De Feyter, P. Leclère, A. P. H. J. Schenning, E. W. Meijer, *J. Am. Chem. Soc.* **2007**, *129*, 9818–9828; d) K. P. van den Hout, R. Martín-Rapún, J. A. J. M. Vekemans, E. W. Meijer, *Chem. Eur. J.* **2007**, *13*, 8113–8123; e) Z. Tomovi'c, J. van Dongen, S. J. George, H. Xu, W. Pisula, P. Leclère, M. M. J. Smulders, S. De Feyter, E. W. Meijer, A. P. H. J. Schenning, *J. Am. Chem. Soc.* **2007**, *129*, 16190–16196; f) Z. Chen, V. Stepanenko, V. Dehn, P. Prins, L. D. A. Siebbeles, J. Seibt, P. Marquetand, V. Engel, F. Würthner, *Chem. Eur. J.* **2007**, *13*, 436–449; g) V. Dehn, Z. Chen, U. Baumeister, P. Prins, L. D. A. Siebbeles, F. Würthner, *Org. Lett.* **2007**, *9*, 1085–1088; h) M. M. J. Smulders, A. P. H. J. Schenning, E. W. Meijer, *J. Am. Chem. Soc.* **2008**, *130*, 606–611; i) H. Wang, T. E. Kaiser, S. Uemura, F. Würthner, *Chem. Commun.* **2008**, 1181–1183.

[21] The morphologies were significantly dependent on the preparation conditions (temperatures on drying, etc.); at least, only unspecific objects, such as spheres, were observed in the dried samples of the gelated materials. Further, spin-coating of the solution at room temp. on glass substrate afforded fibers in the case of free receptors and no morphologies in anion complexes.

[22] F. Rodriguez-Llansola, J. F. Miravet, B. Escuder, *Chem. Commun.* **2009**, 209–211.

[23] Theoretical studies at the AM1 level for **5m2** and **5p2** suggested that the lengths of these receptors in one of the stable conformations were 6.3 and 6.7 nm, respectively (Figure S5 in the Supporting Information).

[24] DLS peak intensities are not always proportional to the amounts of the corresponding aggregates in the solution state. Larger objects often provide fairly intense light scattering in relation to smaller ones, so it is not easy to discuss the quantitative aspects only on the basis of DLS measurements, which may show less strong correlations with UV/Vis absorption spectra.

[25] Extended derivatives based on formyl substituents – dipyrrinpendant acyclic anion receptors, for example – were prepared from **3m1** and **3m2** through subsequent treatment with α-methylpyrrole in the presence of an acid catalyst and DDQ oxidation. Here, in order to exclude axial coordination at Zn^{II} as a bridging metal cation, methyl groups were introduced at the α-positions of the pyrrole rings. Mono- and bis(dipyrrin)-pendant acyclic anion receptors afforded the anion receptors with bis(dipyrrin)Zn^{II} complexes and Zn^{II}-bridged coordination polymers (below), respectively, by treatment with $Zn(OAc)_2$. Such metal-coordination dimers and polymers exhibited anion-responsive behavior in their UV/Vis absorption spectral changes in CH_2Cl_2 upon addition of anions (Figure S11 in the Supporting Information). See also ref.[26]

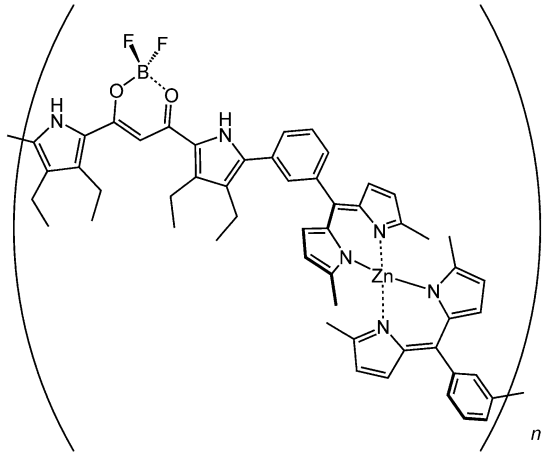

[26] a) H. Maeda, M. Ito, *Chem. Lett.* **2005**, *34*, 1150–1151; b) H. Maeda, M. Hasegawa, T. Hashimoto, T. Kakimoto, S. Nishio, T. Nakanishi, *J. Am. Chem. Soc.* **2006**, *128*, 10024–10025; c) H. Maeda, T. Hashimoto, *Chem. Eur. J.* **2007**, *13*, 7900–7907; d) H. Maeda, T. Hashimoto, R. Fujii, M. Hasegawa, *J. Nanosci. Nanotechnol.* **2009**, *9*, 240–248.

Received: November 23, 2009
Published Online: January 29, 2010

